Optimality and Complexity in Measured Quantum-State Stochastic Processes

Ariadna Venegas-Li[1] · **James P. Crutchfield**[1]

Abstract

If an experimentalist observes a sequence of emitted quantum states via either projective or positive-operator-valued measurements, the outcomes form a time series. Individual time series are realizations of a stochastic process over the measurements' classical outcomes. We recently showed that, in general, the resulting stochastic process is highly complex in two specific senses: (i) it is inherently unpredictable to varying degrees that depend on measurement choice and (ii) optimal prediction requires using an infinite number of temporal features. Here, we identify the mechanism underlying this complicatedness as generator nonunifilarity—the degeneracy between sequences of generator states and sequences of measurement outcomes. This makes it possible to quantitatively explore the influence that measurement choice has on a quantum process' degrees of randomness and structural complexity using recently introduced methods from ergodic theory. Progress in this, though, requires quantitative measures of structure and memory in observed time series. And, success requires accurate and efficient estimation algorithms that overcome the requirement to explicitly represent an infinite set of predictive features. We provide these metrics and associated algorithms, using them to design informationally-optimal measurements of open quantum dynamical systems.

1 Introduction

Time series of controlled quantum states are essential to quantum physics, quantum information and computing, and their implementations in novel technologies. Moreover, as quantum

---

✉ James P. Crutchfield
chaos@ucdavis.edu

Ariadna Venegas-Li
avenegasli@ucdavis.edu

[1] Complexity Sciences Center and Physics Department, University of California at Davis, One Shields Avenue, Davis, CA 95616, USA
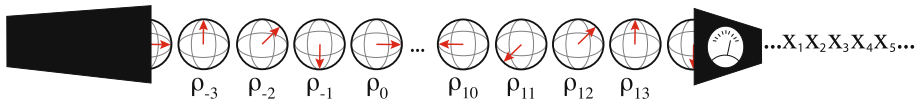
Fig. 1 A general controlled quantum source (CQS) as a discrete-time quantum dynamical system (black box) that stochastically generates a time series of quantum states $\rho_{t-2}\rho_{t-1}\rho_t \ldots$ (density matrices). Measuring each state in the sequence realizes a classical stochastic process over random variables $\ldots X_1 X_2 X_3 X_4 X_5 \ldots$

technologies scale to larger qubit collections that evolve coherently over increasingly longer times, fault-tolerant design and error correction of quantum-state time series become increasingly necessary.

Several fault-tolerant systems and diagnostic tools have been developed assuming quantum processes with uncorrelated noise [1–5]. Unfortunately, progressing beyond those assumptions to more physically realistic non-Markovian, correlated processes has been challenging. To date, error correction for non-Markovian quantum processes can be deployed only in specific cases. Moreover, contemporary theory offers a restricted toolset for quantum process identification and control [6–8].

The following explores one reason for these challenges and limited progress. In short, there is substantially more-complicated statistics and correlational structure embedded in non-Markovian quantum processes and in the classical stochastic processes that result from measurement than currently appreciated. We show how to identify the signatures of these complexities and how to constructively address the challenges they pose.

To ameliorate historical inconsistencies, along the way we give unified definitions of Markov and non-Markov processes. Said most simply, these address the role of memory in a structurally consistent way—a way that also gives access to modern multivariate information theory. Clarity in this is essential to appreciating the structural varieties of complex quantum processes. Lasting progress in complex quantum processes depends on this clarity.

Explicating the structures embedded in quantum processes requires stepping back, to revisit a basic question: How to characterize the stochastic process that results from measuring sequential quantum states? The answer is found in a recently-introduced framework for correlated and state-dependent quantum processes [9]. Notably, its toolkit relies only on classical dynamical systems. The turn to the latter is perhaps unexpected from the perspective of quantum physics, but makes sense given that the goal is to describe the classical data an experimentalist has in hand in the laboratory. Specifically, the tools rely on fundamental results that both reach back more than half a century to early ergodic and stochastic process theories, but also call on contemporary mathematics of dynamical systems—specifically, iterated function systems and their stable asymptotic invariant measures [10–12].

Thus, the objects of study here are time series of sequential quantum systems and the stochastic processes that result from sequentially measuring the state of each one.

Generating a time series of sequential quantum states usually occurs under the control of an experimental apparatus. If control over the apparatus is not perfect or if it undergoes dynamics that are unstable or not fully understood, then the time series of emitted quantum states can be profitably regarded as a stochastic process. It may also be desired for a given application, such as quantum cryptography, that a quantum state process be stochastic.

Figure 1 illustrates this with a black box quantum system that emits a quantum state ρ_t (density matrix) at each time t. We refer to this source as a *controlled quantum source* (CQS) and to its output as a *quantum-state stochastic process* (QSSP). It is important to note here, that a distinct quantum state is emitted at each timestep and the object of study is the time

series of these states. To emphasize, we are not investigating the dynamical evolution of an individual quantum state or individual quantum system.

Continuing from left to right in Fig. 1, measurement of a quantum-state time series results in a stochastic process of classical measurement outcomes. Of that classical process we then ask:

- *Statistics*: What are the properties of this observed classical process—its randomness, correlation, memory?
- *System identification*: What properties of the underlying quantum stochastic generator hidden in the black box can be reconstructed from the observed classical process?
- *Measurement choice*: How does measurement affect the observed statistics and controller identification?

Computational mechanics [13–15] was originally introduced to constructively answer these questions for purely-classical hidden processes. To do this, it extracts the "effective theory" from a time series of observations and provides measures of the time series' randomness and structure. In particular, a process' *statistical complexity* C_μ quantifies how much structure or memory is required to do optimal prediction. And, the *entropy rate* h_μ quantifies a process' intrinsic randomness—the rate of information production.

This toolset, together with the fact that measuring a quantum time series results in a classical time series, motivates our approach. We adapt these classical measures of intrinsic randomness and structure to describe the classical time series observed when applying measurement operators to a time series of quantum states. This provides a description of relevant properties of a stochastic process of quantum states—properties that have proven usefully diagnostic and descriptive in the classical setting. The following endeavors to show that they are for quantum processes. Moreover, our approach allows analyzing the effects that measurement choice has on the observed complexity of a quantum dynamical process.

This serves as a starting point to more fully appreciating the complicatedness of quantum dynamical processes and the role that measurement plays. Over the longer term, building on this, the goal is to characterize stochastic quantum processes beyond being Markovian or non-Markovian—memoryless or memoryful—to arrive at understanding of their informational and statistical properties. These metrics can then support more informed approaches to error correction and to potentially leveraging noise for particular tasks, just as their classical analogs have for thermodynamic computing [16, 17].

Our agenda is as follows. Section 2 motivates the set-up and places the results in the context of the observed stochasticity of quantum systems. It introduces the notion of quantum stochastic processes and information and correlations in quantum time series. The next two sections go into detail on the technical problem statement. First, Sect. 3 describes the general type of QSSP that we study and how we model them. Second, Sect. 4 details how we measure a QSSP and describes the classical stochastic process that results. Section 5 identifies generator nonunifilarity as the mechanism by which quantum measurement induces varying randomness and correlation in the resulting classical process. Section 6 then gives a short summary of the tools required to analyze measured QSSPs. Following that, Sect. 7 applies the methods to example QSSPs and their corresponding measured processes. Section 7.5, in particular, highlights the general properties that can be extracted. Section 8, by way of illustrating the general results, applies the previously introduced metrics to particular examples and investigates their dependence on measurement choice and discusses alternative measurement protocols. This serves as a way to introduce notions of measurement optimality in Sect. 9.

2 Background

To start, let's locate our development in contrast to other quantum settings.

Perhaps the most common setting for quantum processes investigates a single quantum system evolving in time. In this, stochasticity in the system's state evolution arises from its interaction with an environment. Within this setting stochasticity in temporal evolution can also arise from inherent nonlinear dynamics or repeated measurement and other state mappings.

Historically, though, there is a longstanding effort to characterize stochasticity in quantum dynamics as a means to manage quantum noise [18, 19]. Much of the machinery developed to describe quantum stochastic phenomena arose from open quantum systems, seeded around quantum master equations and relying heavily on assuming process Markovity [20, 21]. More recently, an effort emerged to understand, detect, and quantify non-Markovity, and many examples of specific non-Markovian quantum dynamics have been analyzed in detail [6, 7, 22, 23].

From the perspective of Markov's original concept of "complex chains" [24, 25] and the modern theory of (classical) Markov processes, though, these approaches rely on an unnecessarily-varied set of Markovity definitions. One consequence is that, most basically, they do not agree on what process memory and correlation are. This also makes comparing results across investigations challenging. And so, we give and apply a unified definition of memory that addresses classical and measured quantum processes. Appendix B discusses this in more detail, noting the conflicting definitions one finds.

Directly importing the concept of classical stochastic processes to the quantum domain has proved challenging, as Ref. [26] discusses in detail. While there are several causes, the primary difficulty is that the Kolmogorov Extension Theorem—specifying event-sequence probabilities and measures—breaks down when the random variables are quantal and are generated by quantum mechanisms.

Recently, process tensors were introduced to treat such quantum stochastic processes [27–29]. They promise a gateway to probe quantum stochasticity beyond the binary distinction of Markov versus non-Markov. Modeling correlations beyond merely Markovian will allow analyzing a broader class of quantum processes. That said, the endeavor is new.

While there are parallels with process-tensor representations, the following focuses on a different type of dynamical process—different also from individual quantum-system temporal evolution. It considers a sequence of distinct entities, in which the quantum state of each is a random variable at each time step. In this, there is a rough parallel to quantum spin chains. Notably, these variables can be correlated by the physical mechanism that sequentially generates them.

Consider a physical system that emits qubits, each in a state that is noisy or stochastic; for instance, photons emanating from a blinking quantum dot [30]. The difference between these processes and the more-familiar evolving single-system dynamics is that, at each time step, the quantum state of the emitted qubit is its own random variable. That is, each successive random variable lives in its own Hilbert space. The associated random variable takes on a specific qubit state, and measuring these states does not interfere with the quantum process generator nor with other prior or future qubits. In short, as the quantum source emits quantum states the dimension of the product Hilbert space grows. As a consequence, addressing time-asymptotic properties requires working with an infinite product state space. And, these change the kind of investigation we pursue. We investigate time series of quantum states emitted by

a physical system in the spirit of analyzing the multivariate statistical and informational properties of the system's dynamics as developed in Ref. [31].

Specifically, Ref. [9] recently introduced a framework for such quantum-state stochastic processes. It casts the problem of quantum processes in a way that is amenable to directly applying the tools of classical stochastic processes to characterize the informational and structural properties of QSSPs. It showed that a qubit time series, when observed through projective measurements, generically results in a highly complex classical stochastic process. Highly complex here means that the observed process has positive entropy rate and requires an infinite number of temporal features to optimally predict future outcomes. It also demonstrated that measurement choice—the manner in which an observer interacts with a qubit stream—can drive a quantum process appear more or less complex.

To accomplish this, the prequel adapted the metrics of computational mechanics to describe randomness and structure in the measured processes. Section 6 summarizes these metrics. The following takes those results further by introducing an analytical framework to describe stochastic processes over quantum states. It provides a more thorough-going exploration and isolates the physical mechanism—generator nonunifilarity—responsible for the observed complexity. It analyzes a variety of examples that span the possible types of dynamics and offers several avenues for future explorations, including outlining how to optimize measurements of quantum processes to various ends.

3 Quantum-State Stochastic Processes

The following introduces the main objects of study—quantum-state stochastic processes—and the information sources that generate them. It then moves on to explain how the classical processes that emerge "in the lab" are produced through measurement of individual quantum states in QSSP realizations. With the latter processes in hand, it then shows how to quantify their randomness and structure using metrics available from information theory and explores how those properties vary as a function of measurement choice.

3.1 Quantum Processes

Consider a given quantum source that emits a sequence of individual quantum states. At each time step, the quantum state it emits takes on a value from a finite set. We refer to these sources as *controlled quantum sources* (CQSs) and, in their operation, they generate *quantum-state stochastic processes*. We will now define quantum-state stochastic processes.

Let R_t denote the random variable for the quantum state emitted at time t. The realization of R_t as a particular quantum state is $\rho_t \in \mathcal{A}_Q$, where $\mathcal{A}_Q$ is the set of available quantum states in a Hilbert space. The random variable for a sequence of quantum states emitted between times t and $t + \ell$ is denoted by the block random variable $R_{t:t+\ell}$ (inclusive on the left, exclusive on the right). Then $\rho_{t:t+\ell}$ denotes the realized sequence of quantum states.

Definition 1 (*Homogeneous Quantum-State Stochastic Process*) Let $\mathcal{A}_Q \subseteq \mathcal{H}^d$ be the set of available quantum states in the d-dimensional Hilbert space $\mathcal{H}^d$. $\Omega = \mathcal{A}_Q^{\mathbb{Z}}$ is then the space of bi-infinite sequences over $\mathcal{A}_Q$. Consider the probability space $\mathcal{P} = (\Omega, \mathcal{F}, P)$, where $\mathcal{F}$ is the σ−algebra on the cylinder sets of Ω and P a probability measure over the cylinder sets. $R_{-\infty:\infty}$ denotes the discrete-time random-variable sequence of quantum states described by the quantum-state stochastic process $\mathcal{P}$. It comprises the sequences of random variables that take on values according to a measurable function $T_t : \Omega \to \mathcal{A}_Q^t$:

$$R_t = T_t(R_{-\infty:\infty}) \,,$$

for $t \in \mathbb{Z}$.

To emphasize again, we work with distinct physical objects at each time step. That is, each random variable R_t takes a value on its own Hilbert space $\mathcal{H}_t^d$. In a *homogeneous* process the Hilbert spaces are of the same type. Think, for example, of a time series of photons, each photon emitted by a source at a certain time step, in this or that quantum state.

We restrict our study to *stationary* and *ergodic* QSSPs.

Definition 2 (*Stationarity*) A stationary QSSP is one in which the probability of observing a particular sequence of quantum states is independent of the time at which the observation is made. That is, the probability of an observed quantum sequence is time-translation invariant:

$$\Pr(R_{t:t+\ell} = \rho_{t:t+\ell}) = \Pr(R_{0:\ell} = \rho_{0:\ell}) \,, \tag{1}$$

for all $t \in \mathbb{Z}$, $\ell \in \mathbb{Z}$, and $\rho_{0:\ell}$.

Definition 3 (*Ergodicity*) A QSSP is *ergodic* if all long realizations obey the QSSP's statistical properties. That is, given a long realization $R_{0:n} = \rho_{0:n}$, the probability of observing a finite realization of $R_{0:\ell}$ of length $\ell \ll n$ in $\rho_{0:n}$ is the same as observing that same block in multiple realizations of length ℓ drawn from the QSSP.

The following considers only QSSPs satisfying these three definitions. It also imposes two more restrictions. First, it focuses on stochastic processes of qubits, since they are the basic carriers of quantum information. Second, it focuses on processes in which for all t: $\rho_t^2 = \rho_t$. That is, the quantum states realized by the R_ts are strictly pure states, lying on the surface of the Bloch sphere. This rules out (for now) the presence of entanglement within quantum state blocks. And, in practical terms, it means the joint variable over qubits emitted in a time interval can be represented as:

$$R_{t:t+\ell} = R_t \otimes R_{t+1} \otimes \ldots \otimes R_{t+\ell-1} \tag{2}$$

and a realization is both a pure state and the tensor product of the individual pure quantum states:

$$\rho_{t:t+\ell} = \rho_t \otimes \rho_{t+1} \otimes \ldots \otimes \rho_{t+\ell-1} \,.$$

Again, together these definitions describe a setup in which a quantum system emits individual qubits at each time step. The latter are in pure quantum states. The quantum system that emits the qubits is the controlled qubit source (CQS). Occasionally, this is abbreviated as the *controller* to make reference to an experimenter having some level of control, perhaps through design, over qubit emission, which can be stochastic.

3.2 Quantum Sources and Generator Presentations

In short, quantum sources generate quantum processes. Here, we concentrate on a particular implementation of CQSs—those that generate QSSPs via a classical controller with a finite memory in the form of a hidden Markov chain (HMC) [32–34]. (Appendix C provides a short refresher on HMCs.) To illustrate, this means that the black box in Fig. 1 is reified as in the white box shown in Fig. 2: a HMC controlling what the box emits. Correspondingly, we refer to this qubit source as a *classically controlled qubit source* (cCQS).
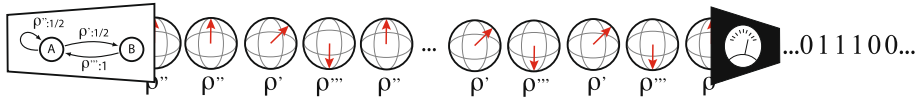
Fig. 2 Classically-Controlled Quantum Source and its Emitted Process: (Left) As the internal hidden Markov controller operates, at each time t the emitted symbols $\mathcal{A}$ (not shown) determine the qubit's quantum state $\rho_t \in \mathcal{A}_Q$. As shown, the latter are realized as density matrices ρ', ρ'', and ρ'''. (For simplicity the controller's emitted symbols $\mathcal{A}$ are not explicitly shown, only the resulting quantum states $\rho \in \mathcal{A}_Q$.) (Middle) The resulting output quantum process is a sequence of distinct $\mathcal{H}^2$ Hilbert spaces, displayed as a series of Bloch spheres with realized state vectors displayed inside. (Right) Measuring each qubit realizes a classical stochastic process . . . 011100

The choice of finite-state HMC controller to model a cCQS is natural, in that HMCs are a standard representation of finite-memory stochastic processes, are widely used to model noisy classical sources and communication channels, and can be fully analyzed [35, 36]. Also, once we complete appropriately developing the present framework, HMCs are easily extended to represent more general sources, such as those driven by quantum controllers [37].

Definition 4 (*Classically-Controlled Quantum Source*) A cCQS is a tuple $(\mathcal{S}, \mathcal{A}_Q, \{\mathbb{T}^\rho\})$ where:

1. $\mathcal{S}$ is the set of hidden states of the HMC controller.
2. Alphabet $\mathcal{A}$ is a finite set of symbols in one-to-one correspondence with the set $\mathcal{A}_Q$ of available qubit quantum states. The latter are emitted by the cCQS when a symbol is encountered on a transition. To simplify notation, both a symbol and its qubit state are denoted by a density matrix $\rho \in \mathcal{H}^2$.
3. $\{\mathbb{T}^\rho : \rho \in \mathcal{A}_Q\}$ is a set of quantum-state labeled transition matrices of size $|\mathcal{S}| \times |\mathcal{S}|$. $\mathbb{T}^\rho_{\sigma\sigma'}$ is the probability of transitioning from internal state σ to internal state σ' (both in $\mathcal{S}$) while emitting symbol (or, effectively, quantum state) ρ.

The labeled transition matrices $\{\mathbb{T}^\rho\}$ sum to the internal-state stochastic transition matrix over hidden states: $\mathbb{T} = \sum_{\rho \in \mathcal{A}_Q} \mathbb{T}^\rho$. This, in turn, determines the HMC's stationary internal-state distribution π as the left eigenvector of $\mathbb{T}$ with eigenvalue 1: $\pi = \pi \mathbb{T}$. π is then a vector of size $|\mathcal{S}|$ in which the entry π_σ represents the asymptotic probability of the HMC being in internal state $\sigma \in \mathcal{S}$.

For an example, see the cCQS in Fig. 3, where:

1. $\mathcal{S} = \{A, B\}$.
2. $\mathcal{A}_Q = \{\rho_\psi = |\psi\rangle\langle\psi|, \rho_\varphi = |\varphi\rangle\langle\varphi|\}$. Here, $|\psi\rangle$ and $|\varphi\rangle$ are pure quantum states.
3. $\{\mathbb{T}^\rho\} = \{\mathbb{T}^{\rho_\varphi}, \mathbb{T}^{\rho_\psi}\}$, where:

$$\mathbb{T}^{\rho_\varphi} = \begin{pmatrix} 0 & 1/2 \\ 0 & 0 \end{pmatrix}$$

$$\mathbb{T}^{\rho_\psi} = \begin{pmatrix} 1/2 & 0 \\ 0 & 1 \end{pmatrix} .$$

4. $\pi = \begin{pmatrix} 2/3 & 1/3 \end{pmatrix}$, the left eigenvector of:

$$\mathbb{T} = \mathbb{T}^{\rho_\varphi} + \mathbb{T}^{\rho_\psi}$$
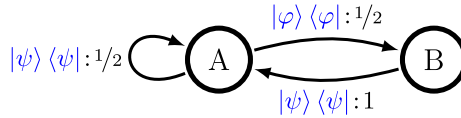$$= \begin{pmatrix} 1/2 & 1/2 \\ 0 & 1 \end{pmatrix} .$$

Fig. 3 cCQS Operation: If the HMC controller is in state A the cCQS has equal probabilities of remaining there or transitioning to state B. If a transition to state B then occurs, the system emits a qubit in the pure state $|\varphi\rangle\langle\varphi|$. In the next time step the cCQS must transition to state A and it then emits a qubit in state $|\psi\rangle\langle\psi|$. That is, the edge labels $\rho : p$ indicate taking the state-to-state transition with probability p and emitting quantum state ρ. As the cCQS operates, a qubit is output at each time step, over time the result is a qubit time series

The following implements cCQSs with finite-memory HMC controllers: $|\mathcal{S}| < \infty$. It also specifies that HMC controller transitions are *unifilar*: The current internal hidden state and emitted quantum state uniquely determine the next internal hidden state.

Section 5.2 gives a more general and detailed account of unifilarity. Section 6 then highlights several of its consequences. As will become clear, the distinction between unifilar and nonunifilar HMCs plays a large role in driving the complexity of quantum processes on their own and when measured.

These choices ensure that the cCQS's randomness and complexity can be directly calculated. And so, the effects of measurement on the quantum process are made most explicit. That said, the analysis below can be applied directly to nonunifilar controllers, with the caveat that the controller's structure and randomness are more complicated to quantify as will be made clear in the following sections.

4 Measured Quantum-State Stochastic Processes

A central aspect of the process realized in the laboratory is how an observer interacts with the QSSP. Naturally, interactions occur via quantum measurement, but there are multiple options for both measurement type and implemented protocol. We now set the stage for measurement protocols and define the specific measurements and protocols used.

4.1 Measurement Protocols

We view a measurement protocol as a communication channel between the quantum stochastic process $R_{-\infty:\infty}$ and its measured companion—a classical stochastic process $X_{-\infty:\infty}$. Denote the relationship between the QSSP random variables and those of the measured process by:

$$X_t = \mathcal{I}_t(R_t) . \tag{3}$$

Where $\mathcal{I}_t$ represents the action of a measurement on the quantum state ρ_t output at time t. The set $\mathcal{I} = \{\mathcal{I}_t\}$ for all t defines a measurement protocol. In a slight abuse of notation, we use the variable $\mathcal{I}_t$ to represent both the measurement channel and the particular measurement operator applied at time t. For short, we refer to the measurement protocol as just $\mathcal{I}$ and denote the relationship between the QSSP and its corresponding measured stochastic process by:

$$X_{-\infty:\infty} = \mathcal{I}(R_{-\infty:\infty}) . \tag{4}$$

To recapitulate the notation, at each time step the random variable R_t takes on the value of a particular quantum state ρ_t. That, in turn, is measured with operator $\mathcal{I}_t$. The resulting

measurement outcome is denoted by the random variable X_t, which takes on a particular value $x_t \in \mathcal{A}_M$, with $\mathcal{A}_M$ the set of possible measurement outcomes.

We now define the basic measurement protocol used.

Definition 5 (*Single State Constant-Measurement Protocol*) As a QSSP is output, each quantum state passes through a measurement channel $\mathcal{I}_t = \mathcal{E}$, for all t. That is, the same measurement $\mathcal{E}$ is applied to each output state individually: $X_t = \mathcal{E}(R_t)$.

Though the following employs only this protocol, we note that it is straightforward to work with measurement protocols for which $\mathcal{I}_t$ depends on time. For example, a measurement scheme in which the measurements alternated between a measurement along the z-axis and a measurement along the x-axis. Or, a potentially more useful protocol is one in which measurements are adaptive, and the $\mathcal{I}_t$s are chosen given the outputs of a subset of past measurements. One approach to the adaptive measurement protocols is described in Ref. [38].

4.2 Projective Measurements

At each time-step, the observer performs a single measurement $\mathcal{E}$ on the quantum state ρ emitted by the controller. This measurement consists of a finite set of nonnegative operators $\{E_x\}$, in which the index $x \in \mathcal{A}_M$ labels the measurement outcomes. The measurement operators sum to the identity: $\sum_{x \in \mathcal{A}_M} E_x = \mathbb{I}$. The probability of measurement outcome x after measuring quantum state ρ is given by $\Pr(x|\rho) = \mathrm{Tr}(E_x \rho)$, where $\mathrm{Tr}(\cdot)$ is the trace.

We concentrate our analysis on single-state projective measurements, in which the operators are orthogonal. This simplifies the basic framework, for now. That said, Sect. 8.2.1 briefly considers single-state protocols with more-general positive operator-valued measurements (POVMs).

Definition 6 (*Projective Measurement on a QSSP*)

A *projective measurement* $\mathcal{E}$ in a dimension d Hilbert space $\mathcal{H}^d$ consists of a set of mutually orthogonal projectors $\{E_x\}$, with $x \in \{0, 1, \ldots d-1\}$, such that $E_x E_y = E_x \delta_{xy}$ and $\sum_x E_x = \mathbb{I}_d$. When the measurement $\mathcal{E}$ acts on a quantum system in state ρ_t, emitted by the QSSP, the outcome is x_t with probability $\Pr(x_t|\rho_t) = \mathrm{Tr}(E_{x_t} \rho_t)$. Applying a projective measurement to every state emitted by the QSSP yields a classical stochastic process over the values of x. We call the set of possible values of x the *measured process alphabet* $\mathcal{A}_M$.

For example, consider a projective measurement of a qubit consisting of two orthogonal measurement operators $\{E_0, E_1\}$. Without loss of generality these can be written as:

$$E_0 = |\psi_0\rangle\langle\psi_0|$$
$$E_1 = |\psi_1\rangle\langle\psi_1| \, .$$

Later, we refer to the set $\mathbf{E} = \{E_i : i = 0, 1, 2, \ldots\}$ of such measurement operators as the *observation basis*.

Let $|\psi_i\rangle \in \mathcal{H}^2$ and $\langle\psi_0|\psi_1\rangle = 0$. When working with qubit projective measurements, it is convenient to parametrize them using Bloch angles as follows:

$$|\psi_0\rangle = \cos\frac{\theta}{2}|0\rangle + e^{i\phi}\sin\frac{\theta}{2}|1\rangle \tag{6a}$$

$$|\psi_1\rangle = \sin\frac{\theta}{2}|0\rangle - e^{i\phi}\cos\frac{\theta}{2}|1\rangle \, . \tag{6b}$$

The resulting measurements are labeled 0 or 1, respectively. Let X_t denote the random variable for the outcome of measuring the state ρ_t at time t and x_t the realized value. In the case of qubit projective measurements $x_t \in \{0, 1\}$. In this way, applying projective measurement protocol to a QSSP produces a binary classical stochastic process. Knowledge of the CQS's controller and the measurement protocol are the basic ingredients needed to analyze the mechanism that generates these classical stochastic processes—the measured processes.

4.3 Measured Processes

By Eq. (4) the classical stochastic process that is realized by measuring the QSSP is the joint distribution $\Pr(X_{-\infty:\infty})$. The specific value x_t taken on by the random variable X_t depends both on the measurement protocol $\mathcal{I} = \{\mathcal{I}_t\}$ with measurement operators $\{E_{x_t}\}$ and the QSSP and its HMC controller. That is, if the random variable R_t takes on the particular value ρ_t at time t, then:

$$\Pr(X_t = x | R_t = \rho_t, \mathcal{I}_t) = \mathrm{Tr}(E_{x_t} \rho_t) \ . \tag{7}$$

Both the measurement protocol and the QSSP can introduce correlations within the classical stochastic process. That is, even if applying a time-independent measurement protocol, such as a constant single-state measurement protocol, the correlations in $R_{-\infty:\infty}$ will yield correlations in $X_{-\infty:\infty}$. However, even if $R_{-\infty:\infty}$ is an independent, identically distributed (IID) process, a time-correlated measurement protocol $\mathcal{I}$ can yield a correlated classical stochastic process.

4.4 Measured Process Presentations

Importantly, in cases where the QSSP is generated by a cCQS, the measured quantum process can be modeled with a unique HMC, as the following demonstrates.

Proposition 1 *Applying a projective measurement protocol $\mathcal{E}$ to a QSSP $R_{-\infty:\infty}$ generated by a finite-state cCQS M results in a measured process $X_{-\infty:\infty}$ given by a finite-state HMC.*

Proof We establish this by directly constructing the HMC presentation. The HMC $\mathbb{M} = \{\mathcal{S}, \mathcal{A}_M, \{T^x\}, \pi\}$ that generates the measured process has the following components:

1. The same set $\mathcal{S}$ of internal states as the HMC that generated the QSSP.
2. A finite alphabet $\mathcal{A}_M$ consisting of each possible measurement outcome.
3. A set of labeled transition matrices $\{T^x\}$ with $x \in \mathcal{A}_M$ such that:

$$T^x = \sum_{\rho \in \mathcal{A}_Q} \mathbb{T}^\rho \Pr(x | \rho, \mathcal{E}) \tag{8}$$

with:

$$\Pr(x | \rho, \mathcal{E}) = \mathrm{Tr}(E_x \rho) \ . \tag{9}$$

4. The same stationary distribution π as the HMC that generated the QSSP.

Definition 7 We refer to the resulting HMC as a *measured cCQS*.

5 Emergent Quantum Complexity

In this way, fixing a cCQS and a measurement basis determines a unique measured cCQS. This HMC accurately describes the classical stochastic process resulting in the lab.

One would hope to directly analyze the statistical properties of the classical process using that HMC. Or, more modestly, to better and more accurately analyze the classical process using the HMC than by simulating repeated realizations over long times to obtain statistics for estimation. The HMC, after all, exactly describes the process, being a presentation (defined shortly).

We demonstrate that this analysis is very far from a straightforward procedure. Moreover, the difficulties are (i) inherent and (ii) generic to quantum measurement. Despite the challenges, though, with care and the right tools in hand one can fully characterize the measured process' properties.

We introduce two classes of HMCs—those that are unifilar (already peripherally introduced above) and those that are not. The following then explains why measurement induces complex statistics. Specifically, the following establishes that (i) nonunifilarity arises in the measured process HMC, (ii) this is generic for projective measurements, and (iii) complex statistics arise in the measured process due to an exponential explosion of the predictive feature set. Along the way, we introduce generative and predictive presentations—those that can be used to produce process realizations and those that, in addition, can be used to optimally predict realizations.

5.1 Presentations

A given stochastic process can be generated by many different HMCs. Each is called a *presentation* of the given process. The essential requirement is that a presentation describes all and only a process' realizations and their probabilities. HMC presentations are either *unifilar* or *nonunifilar*. Unifilarity controls how useful a presentation is to quantitatively analyzing a process.

5.2 Presentation Unifilarity

Definition 8 (*Unifilarity*) An HMC transition is unifilar if the current internal state σ and the emitted symbol x uniquely determine the next internal state σ': $\Pr(\sigma'|x, \sigma) = 1$, for at most one x. That is, there is at most one transition leaving a state for each symbol.

An HMC is *unifilar* if all its transitions are.

When an HMC is *nonunifilar* there is ambiguity in the next state for at least one transition.

It is a notable fact—one motivating the distinction in the first place—that processes generated by finite unifilar HMCs are less (typically much less) complex than those that can be generated only by finite nonunifilar HMCs.

An intuitive way to see why this occurs is the following. Consider a realization of a given process. If it was emitted by a unifilar HMC the realization has a one-to-one or at most one-to-finite correspondence between the observed symbol series and sequences of hidden-state transitions. In contrast, a realization generated by a nonunifilar HMC has a one-to-infinite correspondence between observed symbols and hidden state transitions. The result in this case is that the number of possible of sequences of hidden states that emit a particular sequence of observed symbols grows exponentially with sequence length. In general, a significantly more

complex hidden structure is required to optimally predict processes generated by nonunifilar HMCs.

5.3 Predictors, Generators, and Irreducible Nonunifilarity

A stochastic process' unifilar presentation, up to redundancies in states or transitions, is an optimal predictor. That is, given an HMC hidden state, the probabilities of the next observed symbols are the optimal, most informed prediction of what that next observed symbol will be.

Unifilar HMCs being process predictors contrasts with nonunifilar HMCs which are not predictors. The latter are only generators of process realizations. Moreover, their states are typically poor predictors.

One way to restate the distinction between process predictors (unifilar presentations) and process generators (nonunifilar presentations) is the following. On the one hand, for a unifilar presentation, there is a deterministic relation between the past $x_{-\infty:t}$ and the current hidden state σ_t. That is, $\sigma_t = f(x_{-\infty:t})$, where $f(\cdot)$ is a function; while many pasts $x_{-\infty:t}$ may lead to σ_t. Moreover, for all such pasts, σ_t must have the same conditional distribution $\Pr(X_{t:\infty}|\sigma_t) = \Pr(X_{t:\infty}|x_{-\infty:t})$ of future sequences given the observed past. Since we can use $\Pr(X_{t:t+1}|\sigma_t)$ to predict future observations, we say that the hidden states in a unifilar presentation are *predictive*.

On the other hand, when employing a process' nonunifilar presentation to predict its future $\Pr(X_{t:t+1}|\cdot)$ requires a mixture of distributions $\Pr(X_{t:t+1}|\sigma_t)$ over the presentation's states $\{\sigma_t\}$. In this sense, nonunifilar states are not predictive. Nonunifilar presentations still *generate* the process accurately, since the states and transitions explicitly provide a probabilistic procedure for eventually emitting all of a process' realizations with the correct probabilities.

Starting with any unifilar HMC presentation for a stochastic process, one can eliminate redundancies in information about the past by merging states σ_t with identical future probability distributions $\Pr(X_{t:\infty}|\sigma_t)$. Eliminating these redundancies gives a unique minimal optimal predictive HMC for a stochastic process. This canonical presentation is called a process' ϵ-machine [13, 15]. The ϵ-machine states are a process' *causal states*. They are causal is the sense that they give the minimal mechanism that allows one to exactly predict process realizations.

Looking ahead, we must distinguish between processes with finite predictive presentations and those without. And, this we can now do.

Definition 9 A stochastic process is *irreducibly nonunifilar* if it is generated by a finite nonunfilar HMC, but there exists no finite unifilar HMC presentation that predicts it.

5.4 Measurement-induced Nonunifilarity

With this background, the tools are in place to address the origins of measurement-induced complexity in observed quantum-state stochastic processes. First, we identify the emergence of nonunifilarity. Second, we argue this happens frequently and, in fact, is generic in measured QSSPs. Third, we explore the consequence—explosive complexity. Finally, we identify the underlying mechanism driving this in quantum state indistinguishability.

Proposition 2 *Quantum measurement of a QSSP generated by a cCQS can lead to a classical process represented by a nonunifilar measured cCQS.*

Proof Consider cCQS hidden state σ with outgoing transitions to two distinct hidden states σ_I and σ_{II}. The first transition emits quantum state ρ' and the second, ρ''. Now, performing a measurement $\{E_0, E_1\}$ on the emitted quantum states, both measured transitions have nonzero probability of emitting the same symbol. Recall from Eq. (8):

$$T_{\sigma\sigma'}^x = \sum_{\rho \in \mathcal{A}_Q} \mathbb{T}_{\sigma\sigma'}^\rho \Pr(x|\rho) \ .$$

Note that above and in what follows we suppress explicit mention of the measurement protocol in the conditional probabilities, simplifying $\Pr(x|\rho, \mathcal{E})$ *to* $\Pr(x|\rho)$ for ease of notation. Now, consider a ρ that gives a nonzero probability of obtaining measurement outcome x. Note that this is the case for $\sigma' = \sigma_I$ and $\sigma' = \sigma_{II}$. Then, as long as $\mathbb{T}_{\sigma\sigma'}^\rho$ is nonzero for this ρ, both $T_{\sigma\sigma_I}^x$ and $T_{\sigma\sigma_{II}}^x$ will be nonzero. This makes the observed transition out of state σ nonunifilar and, thus, makes the measured cCQS nonunifilar.

The implications become more apparent later, when discussing how HMC nonunifilarity almost always implies that the process it generates is irreducibly nonunifilar. In this way, measurement can—and as discussed later, almost always will—induce irreducible nonunifilarity of the measured process.

5.5 Nonunifilarity is Generic

We say a property is *measurement generic* over a set of measurements—for instance, qubit projective measurements—if it holds true for almost all measurements but a measure zero subset. Similarly, a property is *source generic* if it holds true for the QSSPs generated by almost all cCQSs.

Proposition 3 *A measured cCQS HMC is generically nonunifilar. This is true both source generically and measurement generically over the set of projective measurements.*

Proof Consider the constraints that give rise to unifilar transitions. Recall the entries of the labeled-transition matrices for a measured cCQS, as defined in Eq. (8):

$$T_{\sigma\sigma'}^x = \sum_{\rho \in \mathcal{A}_Q} \mathbb{T}_{\sigma\sigma'}^\rho \Pr(x|\rho) \ .$$

Each entry is composed of a sum of terms. For the measured cCQS to maintain unifilarity there should be at most one nonzero term per row of each labeled transition matrix. That is, for each $x \in \mathcal{A}$ and $\sigma \in \mathcal{S}$ pair, the term $T_{\sigma\sigma'}^x$ is nonzero for at most one value of σ'.

For unifilarity to hold, the following conditions on the underlying cCQS and measurement must be satisfied:

1 A hidden state with an outgoing transition to only one other hidden state maintains unifilarity.
2 All cCQS hidden states can have at most two outgoing transitions (to distinct states). Denote the quantum states emitted on the outgoing edges ρ_a and ρ_b and the two destination states σ_a and σ_b, respectively. Thus, for each cCQS hidden state σ there are at most two nonzero transition elements: $\mathbb{T}_{\sigma\sigma_a}^{\rho_a}$ and $\mathbb{T}_{\sigma\sigma_b}^{\rho_b}$, say. When determining the measured cCQS's labeled transitions $T_{\sigma\sigma'}^x$, for each σ and x, there will be at most two contributions. The following condition ensures that these two contributions do not result in two or more nonzero values for each σ.

3 If the state has two outgoing transitions then, to maintain unifilarity, it must satisfy:

- The two emitted quantum states ρ_a and ρ_b on the outgoing transitions must be orthogonal to each other.
- The measurement basis must be aligned with ρ_a and ρ_b. That is, each measurement operator must project into the quantum states that the process emits—ρ_a and ρ_b.

For a given pair of x and σ, these ensure that the only potentially nonzero terms are $T_{\sigma\sigma_a}^{\rho_a}$ and $T_{\sigma\sigma_b}^{\rho_b}$. If the projective measurement with outcome x is aligned with either ρ_a or ρ_b, however, then only one of the terms of the form $\mathbb{T}_{\sigma\sigma'}^{\rho}\mathrm{Pr}(x|\rho)$ can be nonzero for a given ρ. And so, there will be at most one nonzero term in the σ row of transition matrix T^x. This guarantees that the measured cCQS remains unifilar.

Conditions 1, 2, and 3 are highly restrictive in the space of cCQSs. That is, almost none of the possible labeled transition matrices $\mathbb{T}^{\rho}$ satisfy them. In turn, this means that measured cCQSs are source-generically nonunifilar.

For a given cCQS, Condition 3 is highly restrictive in the set of projective measurements and is only satisfied for one measurement choice out of a continuous set of possible measurement choices. Therefore, the measured cCQS is measurement-generically nonunifilar.

It is also important here to note that Conditions 2 and 3 refer to the case in which the cCQS emits qubits. For a cCQS that emits qudits, these conditions can be generalized to allow for d distinct transitions to other states. The generalization is straightforward: To maintain unifilarity the output quantum states associated with those d transitions must be mutually orthogonal and the measurement chosen must be able to distinguish perfectly between those d states.

As Sect. 5.7 develops in more detail, Prop. 3 says that measured processes are typically highly complex, in the sense that they generically have an uncountable infinity of predictive features (causal states), divergent statistical complexity, and a positive entropy rate.

5.6 Variations

Several observations are in order on generic nonunifilarity for qubit processes and how generic nonunifilarity trades-off against the Hilbert space dimension of the QSSP's quantum states.

Structurally, a binary alphabet highly restricts the possibilities for a particular HMC's topology to support unifilarity. This could lead to a rushed conclusion that restricting to projective measurements plays a determinant role in nonunifilarity of measured quantum processes. In fact, however, allowing for POVMs does not change this aspect. Suppose a particular cCQS hidden state has two outgoing edges with nonorthogonal quantum states ρ_a and ρ_b. In any POVM with two or more measurement operators at least one has a nonzero probability of being an outcome when applied to both ρ_a and ρ_b. This means that in the measured cCQS there are at least two distinct outgoing transitions with the same symbol. And, this again yields nonunifilar dynamics. Section 8.2.1 explores this for an example POVM measurement protocol.

In general, when the quantum states emitted by the cCQS are restricted to qubits, the relatively low dimensionality of the Hilbert space means that we generically recover nonunifilar machines. This is due to the fact that the only case in which a measurement with two or more operators (not necessarily projectors) can perfectly distinguish between two quantum states is when they are orthogonal. (Distinguishing quantum states here means that none of the operators have nonzero probability to be the measured outcome on both of the quantum

states.) And, even in this case, distinguishability holds only for a particular measurement basis that aligns with the two orthogonal states to measure.

The second observation concerns a potentially-useful generalization of how to reduce nonunifilarities in higher dimension. The preceding establishes that irreducible nonunifilarity dominates in measured QSSPs, and this is true generically. However, if the quantum states emitted by the cCQS are qudits, there is more "room" to reduce the nonunifilar transitions in the measured cCQSs when the Hilbert space dimension is larger than $d = 2$. For instance, when the number of outgoing transitions from one hidden state to distinct hidden states is at most d, one can partition the set of quantum states emitted in those transitions into mutually orthogonal subsets. In that case one can devise a measurement that captures each orthogonal subset as a distinct measurement outcome. This, in a sense, constrains the nonunifilarities to be only in the outgoing transitions that have output quantum states with nonzero overlap. Effectively, the measured cCQS loses information about which specific state was output within each orthogonal subset by turning those into nonunifilar transitions, but maintains the information about which output states where mutually orthogonal. This somewhat reduces the complexity of the measured cCQS.

As a simple example, consider a cCQS that outputs qutrits. A particular hidden state has three outgoing edges to distinct states, each outputting qutrits in states $|0\rangle$, $|+\rangle$, and $|2\rangle$. One can devise a measurement that outputs 0 if the qutrit is in the subspace spanned by $|0\rangle$ and $|1\rangle$, and outputs 1 if the qutrit is orthogonal to that subspace. In this case the measured cCQS has nonunifilarity only in the $|0\rangle$ and $|+\rangle$ transitions. This reduction of nonunfilarity is only viable as long as there is an orthogonal subset within the set of possible output states $\mathcal{A}_Q$. So, it is still rare, but the larger the Hilbert space of output states is, the more opportunities there are for reducing nonunifilarity.

Naturally, these measurements should also be physically motivated by the information the experimenter is trying to extract from the underlying quantum dynamic. Thus, when working with quantum information from a classical reality, there is a tradeoff between the complexity of the observed dynamics and how coarsely or finely one probes the quantum state through measurement. Compared to general qudits, the space of qubits offers much less room for coarser measurements.

The practical upshot of these arguments is that analyzing a measured cCQS requires working with nonunifilar presentations of the observed classical stochastic process.

5.7 Explosive Complexity

Consider a process that is generated by a finite nonunifilar presentation. One can construct a unifilar presentation for it. The reasons for doing so will become abundantly clear shortly. For now, say a predictive presentation is needed. The states of the unifilar presentation are Black-well's *mixed states* [39]. These are identified using the *Mixed State Algorithm* introduced in Refs. [40, 41] and explained in detail in Ref. [10]. Said simply, by tracking the "states of knowledge" about an HMC's internal states as revealed indirectly by emitted symbols, one builds a unifilar hidden Markov chain whose states are the mixed states and whose transitions are the mixed-state to mixed-state transitions. The result is known as the process' *mixed state presentation* (MSP). The MSP then provides an insightful and calculationally efficient way to determine many, if not all, of a process' statistical and informational properties.

Appendix E reviews MSP construction and its properties, here we summarize. Given a process' N-state HMC presentation M, one constructs M's set $\mathcal{R}$ of mixed states as the conditional probability distributions $\eta(x_{-\ell:0}) = \Pr(\mathcal{S}_0 = \sigma | X_{-\ell:0} = x_{-\ell:0})$ over the HMC's

hidden states $\sigma \in \mathcal{S}$ given all possible sequences $x_{-\ell:0} \in \mathcal{A}^\ell$. Given M and an observed symbol sequence $x_{-\ell:0}$, there is a unique mixed state $\eta(x_{-\ell:0})$ that represents the best guess as to M's current internal state. Moreover, the set of the process' allowed sequences of all lengths $\ell \in \mathbb{N}$ induces a invariant measure μ on the state distribution $(N-1)$-dimensional simplex. We simply denote this as the *mixed state distribution* $\mu(\mathcal{R})$. An HMC's mixed state set $\mathcal{R}$ together with the transition dynamic $\mathcal{W}$ between mixed states induced by observed sequences form the HMC's MSP: $\mathrm{MSP}(M) = \{\mathcal{R}, \mathcal{W}\}$.

Importantly, by construction an HMC's MSP is a unifilar presentation of the stochastic process generated by the HMC. Additionally, the set of mixed states $\mathcal{R}$ corresponds to the process' set of causal states. The consequence is that the MSP, up to minimizing state redundancies, is the unique optimally predictive model of the stochastic process—its ϵ-machine [11].

Conjecture 1 *A process generated by a nonunifilar presentation generically is an irreducibly nonunifilar stochastic process. That is, it requires an infinite number of predictive features (causal states) for optimal prediction.*

Blackwell introduced this conjecture in his seminal 1957 work on classical stochastic processes [39]. There, he developed several of the first information-theoretic results for what he called *functions of Markov chains*. These are equivalent to what are nowadays called hidden Markov chains. Moreover, for very specific cases Blackwell showed that the set of (predictive) features that a process stores from observed sequences can be finite or countable. In all other instances, the predictive features set is uncountably infinite. These predictive features are equivalent to the process' MSP mixed states $\mathcal{R}$. The primary lesson is that the predictive complexity of irreducibly nonunifilar processes explodes, despite them being generated by a finite mechanism—a finite-state HMC.

Long experience and extensive explorations of HMC space support Blackwell's claims and this conjecture, which has also been recorded elsewhere [9–11, 42, 43]. Reference [12] goes into great detail about the mechanisms by which these stochastic processes generate and process information. It reviews the arguments and evidence that the conjecture holds quite broadly. Finally, for measured cCQSs we have not encountered a single violation. That said, establishing the conjecture for the general or the quantum settings remain open problems.

5.8 Quantum State Indistinguishability

Section 5.5 detailed the structural reasons that make measured cCQSs generically nonunifilar. Behind these lies a simple physical property that is responsible for irreducible nonunifilarity and, thus, explosion in complexity of measured quantum processes. When applying a measurement to a QSSP that emits qubits in two or more distinct quantum states, a single measurement will generally have a nonzero probability of not being able to distinguish which quantum state it measured. This indistinguishability between quantum states therefore acts as a source of noise. And, this makes direct reading of the QSSP's underlying structure markedly more memory intensive. This, in turn, radically increases the predictive complexity of the measured process with respect to the QSSP.

One can quantify how distinguishable or indistinguishable two quantum states are using the trace distance [44] for instance. If a particular hidden state in a cCQS has outgoing transitions to two distinct hidden states that emit two different quantum states, a measurement makes the distinction ambiguous (noisy) unless the trace distance between the two quantum states is unity. In that case, the quantum states have orthogonal supports. Moreover, there is the

further requirement for not inducing nonunifilarity that the measurement distinguish between the two states. If these criteria are met, then nonunifilarity in the measured process is not created and there is no explosion in predictive complexity. However, these criteria are very restrictive and so explosive complexity is to be expected in measured cCQSs.

6 Measured Quantum Process Randomness and Structure

Simply establishing explosive complexity is insufficient. One needs yardsticks for analysis and comparison. This section introduces metrics for quantifying randomness and structure in the classical stochastic processes resulting from measured QSSPs. The mathematics for these metrics depend critically on the stochastic process presentation, whether it is unifilar or nonunifilar. The latter is particularly relevant, as the above showed that the measured processes are overwhelmingly irreducible nonunifilar. We begin introducing entropy rate and statistical complexity and how to compute them from unifilar HMCs. The bulk of the effort and interest, though, arise in adapting these to nonunifilar presentations, which follows shortly.

6.1 Unifilar Generators

When an HMC is unifilar, there is a one-to-one or one-to-finite correspondence between a sequence of observed symbols and the sequence of hidden states that generated it. This allows direct, closed-form calculation of process intrinsic randomness and predictive memory from the HMC's internal Markov chain.

6.1.1 Information Creation

Process randomness—the rate at which the process generates information—is quantified through the Shannon *entropy rate* h_μ. It is defined directly for a process, but the useful goal is to obtain short cuts—expressions in terms of a presentation's states and transitions.

Definition 10 A process' *entropy rate* is [45]:

$$h_\mu = \lim_{\ell \to \infty} \frac{\mathrm{H}[X_{0:\ell}]}{\ell} \; , \tag{10}$$

where $\mathrm{H}[X] = -\sum_x \Pr(X = x) \log_2 \Pr(X = x)$ is the Shannon block entropy [31].

That is, h_μ is the average uncertainty per observed symbol. Or, said differently, it quantifies how much information an observer gains asymptotically with each newly measured symbol.

Reference [10] explores in detail how to compute the entropy rate of a process generated by a given HMC. Here, we summarize.

For unifilar HMCs, Shannon [45] showed the entropy rate is exactly computable in closed-form from the HMC's transition matrices and stationary state distribution π:

$$h_\mu = -\sum_{\sigma \in \boldsymbol{\mathcal{S}}} \pi_\sigma \sum_{x \in \mathcal{A}} \sum_{\sigma' \in \boldsymbol{\mathcal{S}}} T_{\sigma\sigma'}^{(x)} \log T_{\sigma\sigma'}^{(x)} \; . \tag{11}$$

This is the state-averaged transition uncertainty. The stationary state distribution is determined by the left eigenvector (associated with eigenvalue 1 and normalized in probability) of the internal state transition matrix $T = \Sigma_{x \in \mathcal{A}} T^{(x)}$.

6.1.2 Information Storage

To quantify the structure of a process' presentation M, the most straightforward measure is its number $|\mathcal{S}|$ of hidden states. Beyond that, a more insightful metric is the amount of historical memory or information the presentation states contain. This is given by the Shannon entropy of the state distribution:

$$H[\mathcal{S}] = -\sum_{\sigma \in \mathcal{S}} \pi_\sigma \log_2 \pi_\sigma .$$ (12)

It quantifies how much information the hidden states store about past observations. That is, it measures how much memory a given HMC has. And, since unifilar presentations are predictors, $H[\mathcal{S}]$ is an upper bound on the amount of information one must maintain on average to optimally predict the process. This upper bound will typically overestimate the memory of the process unless M is a minimal optimal predictive presentation.

For these metrics to describe actual properties of the stochastic process in question and not those of a particular HMC presentation—that, say, could have an overly-large and redundant set of states—we use a process' ϵ-machine, reviewed in Appendix D. In brief, a process'ϵ-machine is its minimal optimal predictive HMC [13–15].

The ϵ-machine's hidden states are a process' *causal states* since they optimally capture the process' causal structure. With them one can make the most accurate predictions of future symbols and their associated probabilities while using minimal memory. The memory in the causal states is then the minimal amount of information from the past that must be stored in hidden states to optimally predict the future.

Definition 11 A stochastic process' *statistical complexity* C_μ is the Shannon entropy of its ϵ-machine's causal states $\mathcal{S}$:

$$\begin{aligned} C_\mu &= H[\mathcal{S}] \\ &= -\sum_{\sigma \in \mathcal{S}} \Pr(S = \sigma) \log_2 \Pr(S = \sigma) . \end{aligned}$$ (13)

C_μ is the minimal memory required to optimally predict the future.

6.2 Nonunifilar Generators

If the only description available for a measured QSSP is a nonunifilar HMC presentation, though, then quantifying the process' stochasticity and structure becomes markedly more complicated due to the explosive complexity demonstrated above. And, this has substantial practical consequences. In the case of intrinsic randomness, Eq. (11) overestimates the entropy rate. In the case of structure, the Shannon entropy of the nonunifilar HMC's hidden states only quantifies the memory used by that particular (likely nonunique) presentation. More to the point, it does not provide information on how much memory is minimally required to *optimally* predict the process.

And, if these challenges were not enough, there is yet another complication at this stage. While constructing the MSP from a process' nonunifilar HMC produces a unifilar HMC, it is rarely finite-state. As we showed, the typical case is an infinite-state HMC, generically with uncountably infinite states [10, 42, 43]. Generally then, the ϵ-machine, the minimized MSP, has an uncountable set of causal states. As a consequence, the statistical complexity of Eq. (13) diverges and the expression for entropy rate in Eq. (11) becomes inadequate.

6.2.1 Information Creation

Reference [10] showed that the correct expression for the process' entropy rate is an integral of the transition uncertainty over the mixed-state simplex $\mathcal{R}$ weighted by the invariant measure $\mu(\eta)$:

$$h_\mu^B = - \int_{\mathcal{R}} d\mu(\eta) \sum_{x \in \mathcal{A}} \Pr(x|\eta) \log_2 \Pr(x|\eta) . \qquad (14)$$

(The B superscript here is a nod to Blackwell's contribution.)

As introduced in Ref. [10], general contractivity of the MSP dynamic $\mathcal{W}$ on the simplex and ergodicity allow accurately evaluating the integral expression. This is implemented by taking an average over a time series of mixed states η_t, rather than integrating over the Blackwell measure $\mu(\eta)$. This yields the process' entropy rate:

$$\widehat{h_\mu^B} = - \lim_{\ell \to \infty} \frac{1}{\ell} \sum_{x \in \mathcal{A}} \sum_{i=0}^{\ell} \Pr(x|\eta_i) \log_2 \Pr(x|\eta_i) , \qquad (15)$$

where $\Pr(x|\eta_i) = \eta(x_{0:i}) \cdot T^{(x)} \cdot \mathbf{1}$, $x_{0:i}$ represents the first i symbols of an arbitrarily long sequence $x_{0:\ell}$ generated by the process' MSP, and $\mathbf{1}$ is a column vector of all ones.

6.2.2 Information Storage

To quantify the structure and memory in these infinite-state processes, not all is lost due to C_μ's divergence. While the latter is generally the case, we can quantify the divergence rate with the *statistical complexity dimension d_μ* of the Blackwell measure $\mu(\eta)$ on $\mathcal{R}$ [11]:

$$d_\mu = - \lim_{\epsilon \to 0} \frac{H_\epsilon[\mathcal{R}]}{\log_2 \epsilon} . \qquad (16)$$

This tracks the rate at which the memory requirements for optimal prediction grow with increasing precision $- \ln \epsilon$. Specifically, $H_\epsilon[Q]$ is the Shannon entropy of the continuous-valued random variable Q coarse-grained at size ϵ. Evaluating d_μ is not a simple matter, though. The procedure is presented in detail in Refs. [11, 12]. In particular, Ref. [12] introduces the *ambiguity rate*, which quantifies the rate at which optimal predictive models discard information by introducing uncertainty over the infinite past. The difference between the entropy rate and the ambiguity rate in a process is fundamental to determine its statistical complexity dimension, as well as the cardinality of its set of mixed states $\mathcal{R}$. The following sections use these methods, suitably adapted to the present quantum setting.

To give a firmer, even visual, grounding to the preceding results and metrics, the next section explores three examples representative of distinct classes of measured cCQSs and how the above metrics characterize them.

7 Classifying Measured Quantum Processes

The metrics for randomness and structure of a measured quantum process depend on the cardinality of the mixed state set $\mathcal{R}$ generated by the measured cCQS. There are three distinct classes: processes for which the number of mixed states is finite, countably infinite, and uncountably infinite. The following examples illustrate processes in these classes.
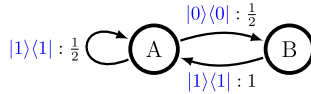
Fig. 4 Unifilar presentation for the *Observation Basis Golden Mean (OB-Golden Mean) process*: A simple cCQS
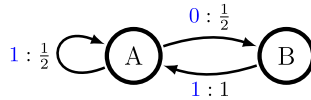

Fig. 5 Measured cCQS of the stochastic process resulting from measuring the quantum process generated in Fig. 4 in the observation basis
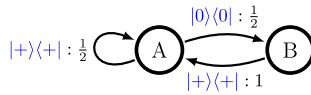

Fig. 6 Structurally, this cCQS is similar to that in Fig. 4. However, not all emitted quantum states are orthogonal. This guarantees that the measured process is more complex, as Fig. 7 shows

7.1 Finite-State

The first quantum process is generated by the unifilar cCQS shown in Fig. 4. It consists of all random sequences without consecutive $|0\rangle\langle 0|$s. Measuring in the observation basis $E_0 = |0\rangle\langle 0|$ and $E_1 = |1\rangle\langle 1|$) yields a unifilar HMC that generates the *Golden Mean Process* consisting of all random sequences without consecutive 0s. Figure 5 shows its minimal presentation—its ϵ-machine: a unifilar HMC with two states. Being unifilar one readily calculates that it has an entropy rate of $h_\mu = 2/3$ bits/symbol from Eq. (11) and a statistical complexity of $C_\mu = 0.918$ bits from Eq. (13).

Although unnecessary in this case, computing the MSP of this presentation—or any other finite unifilar HMC, for that matter—results in an HMC with a finite number of states. In the present case both the measured process' entropy rate and the statistical complexity are finite. They are readily computed via Eqs. (11) and (13), respectively.

Section 5.5 showed that quantum processes in this class are relatively rare in the space of measured cCQSs. They occur only under very constrained circumstances. This observation will become clearer as we consider more complex classes.

7.2 Countably-Infinite-State

The next quantum process is generated by the cCQS in Fig. 6. This is a seemingly slight variation on the previous example. Now, the quantum alphabet $\mathcal{A}_Q$ consists of nonorthogonal states. Instead of emitting quantum states in the observation basis, this cCQS emits qubits in state $|0\rangle\langle 0|$ and others in state $|+\rangle\langle +|$. In this, we define $|+\rangle$ and $|-\rangle$ in the conventional way: $|\pm\rangle = (1/\sqrt{2})(|0\rangle \pm |1\rangle)$. When the process generated by this cCQS is measured in the basis $E_0 = |+\rangle\langle +|$ and $E_1 = |-\rangle\langle -|$, the measured cCQS has the HMC presentation shown in Fig. 7.

Notice, though, that Fig. 7's measured cCQS is nonunifilar. Specifically, knowledge of being in state A and emitting a 0 does not determine the next HMC state. The next state could be either A or B. Thus, to compute the entropy rate for this process one must construct its
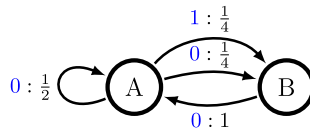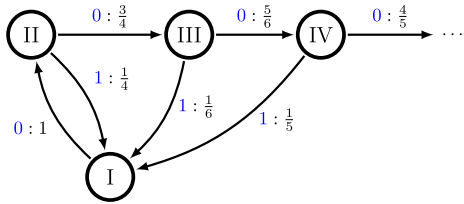
Fig. 7 Measured cCQS for the process generated by measuring the quantum process generated by the cCQS in Fig. 6. This HMC is nonunifilar: if in state A and emitting a 0, the next hidden state may be A or B

Fig. 8 Mixed state presentation of the process generated by Fig. 7's measured cCQS

MSP. The latter is shown in Fig. 8. It has a countable infinity of causal states. Helpfully, as annotated there, the state transition probabilities can be parametrized analytically.

Using Fig. 7 one can follow the logic for constructing the MSP. Independent of any knowledge of the HMC state, seeing symbol 1 the observer concludes with absolute certainty that the measured cCQS is in state B. This is what we referred to previously as a state of knowledge (or a mixed state) represented by hidden state I in Fig. 8. In point of fact, the mixed state associated with state I is $\eta(1) = (0, 1)$. After that, observing symbol 0 or a sequence of 0s means that the measured cCQS has a certain probability of being in each cCQS state A or B. Each additional observation of a 0 then updates the present state of knowledge to one of the mixed states II $= \eta(10)$, III $= \eta(100)$, IV $= \eta(1000)$, ... depending on how many 0s are observed before seeing a 1, when the MSP resets to state I $= \eta(100\ldots01)$.

The measured process' entropy rate can be computed from the HMC in Fig. 7 using the methods for nonunifilar HMCs described in Sect. 6.2. Note, though, that for processes whose MSP has a countable infinity of states, as here, a more rudimentary, though convergent and accurate, approach is available.

When observing the stochastic process, the probability of observing consecutive 0s diminishes with the length of the observed sequence. One then approximates the process' HMC by truncating the MSP at a finite number N of mixed states and then exploring the limiting behavior of both h_μ and C_μ from those unifilar machines as $N \to \infty$. For the example in question, this analysis is illustrated in Fig. 9. One finds that $h_\mu = 0.599$ bits/symbol and $C_\mu = 3.69$ bits. Note that, although infinite state, the process statistical complexity is finite. This is due to the fact that the asymptotic state distribution π decays exponentially fast for mixed states reached via increasingly more 0s.

7.3 Uncountably-Infinite-State

The preceding two processes are relatively simple, in that they all exhibit a finite or countable set of mixed states. In the typical case, as argued in Sect. 5, the measured cCQS has an HMC presentation that is nonunifilar and an MSP with an uncountable infinity of states. Section 5.5 established that this is the typical case for processes generated by cCQSs of two or more states.
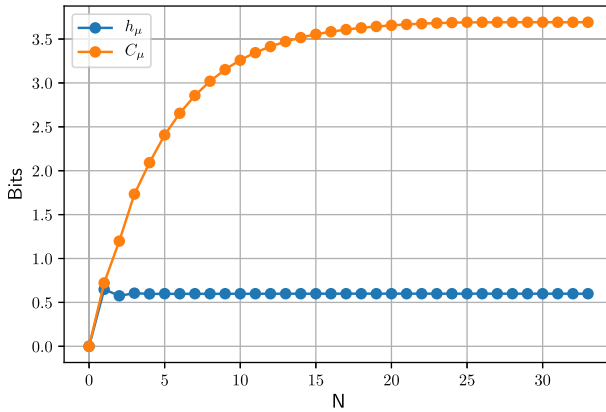
Fig. 9 Entropy rate h_μ (blue) and statistical complexity C_μ (orange) of N-state HMC approximations of the MSP shown in Fig. 8. Notice that h_μ converges rapidly, while C_μ has a stronger dependence on the number of states, but stabilizes around $N = 25$. The values obtained are $h_\mu = 0.599$ bits/symbol and $C_\mu = 3.69$ bits

Fig. 10 Nonorthogonal Nemo Quantum Process: Three-state cCQS that emits qubits in states $|0\rangle\langle0|$ and $|+\rangle\langle+|$
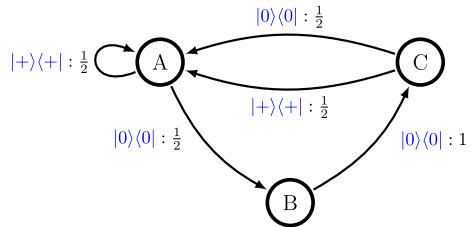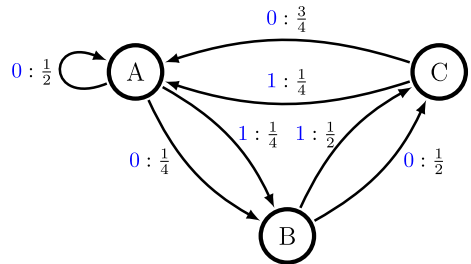

Fig. 11 Measured cCQS presentation of the stochastic process produced when measuring the quantum process generated by Fig. 10's cCQS measured in the observation basis

To illustrate, consider the cCQS of Fig. 10, chosen to have three states principally to aid visualizing the MSP's complexity. The cCQS is then measured in the observation basis, which yields the measured cCQS of Fig. 11.

Note that, as in the example of the countably-infinite state process, the measured cCQS has only a single source of nonunifilarity: the successor state is ambiguous when observing symbol 0 with the HMC in state A. More generally, however, none of the symbols 0 or 1 allow the observer to "synchronize" to the process. That is, observation of a particular symbol does not give an observer certainty in the measured cCQS's state. As argued above mathematically and as is now constructively clear in Fig. 12, this effectively translates into the fact that the MSP of the measured quantum process has an uncountable infinity of mixed states. The MSP—these states together with their transition probabilities—are a markedly less tractable presentation than in the previous two quantum processes.

Fig. 12 MSP's asymptotic invariant measure $\mu(\eta)$ in the mixed-state simplex $\mu(\eta)$. Each mixed state is a point of the form (p_A, p_B, p_C) with p_σ the probability of being in state σ of the measured cCQS in Fig. 11

$(0, 0, 1)$

$(1, 0, 0)$ $(0, 1, 0)$
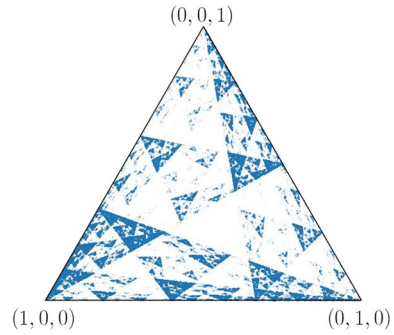
The MSP with all of its states and state transitions cannot be explicitly displayed as with the previous HMCs. Nonetheless, Fig. 12 gives a sense of the MSP's structure and complexity. It presents a plot of 2×10^6 MSP states in the mixed-state simplex $\mathcal{R}$. In fact, it shows $\mu(\eta)$ and its variation in probability density via a histogram with a coarse-graining of 1000×1000 bins.

The measured process' entropy rate is computed using Eq. (15) and has a value of $h_\mu = 0.8896$ bits/symbol. The statistical complexity dimension d_μ of Eq. (16) is computed as described in Refs. [11, 12]: $d_\mu = 1.38$.

7.4 Remarks

As seen from the three examples above, the cardinality of the mixed state set of the distinct measured stochastic processes can vary from a finite state set to a countable infinity of states and on to an uncountable infinity of states. This cardinality affects the way in which the metrics of randomness and structure for the process are computed, but also the values they can take.

For processes with finite sets, the statistical complexity and the entropy rate will generally be finite positive values. This implies that these processes have a certain degree of stochasticity, but that they can be optimally predicted with finite memory resources.

Notably, excepting very special cases, this is also true for processes whose mixed state set has a countably-infinite number of states, as in the second example. These processes have positive entropy rate, signaling that they have an intrinsic degree of randomness. And, while they do require an infinite number of causal states to optimally predict, these states are structured such that one can simulate an optimal predictor of arbitrary precision with a finite amount of memory.

The third case is significantly more complicated than the previous two. A mixed-state presentation with an uncountable infinity of states implies that the statistical complexity of the process diverges. This means that it takes infinite memory to optimally predict these processes. That said, there is an asymptotic invariant measure over the mixed states in $\mathcal{R}$. And, by being able to compute these measures, one can then estimate the process' entropy rate h_μ and also the growth rate d_μ of the memory required for optimal prediction.

This third case, of processes with MSPs that have an uncountably infinite number of states, turns out to be the norm for MSPs of measured cCQSs, as argued above and as we elaborate shortly below. The implications of this are that, in general, the classical processes that we recover from measuring QSSPs generated by cCQSs are highly complex and require infinite memory for optimal prediction. That is, measuring a QSSP greatly obscures the underlying

quantum stochastic process. Fortunately, we have metrics to characterize these processes and to develop a quantitative understanding of how measurement affects the measured quantum processes.

7.5 Genericity of Complexity

The tools are in place now to quantitatively analyze the measured QSSPs that are represented by measured cCQSs. Here, we use the tools to draw broader conclusions about what one should expect and how measurement choice changes the randomness and complexity of measured quantum processes.

The main lesson from the preceding is that one expects explosive complexity and this is reflected in the information-theoretic metrics of the measured process.

Proposition 4 *A measured quantum process, with a measured cCQS presentation, generically is highly complex in two specific ways: it has nonzero entropy rate and statistical complexity dimension. That is, it requires uncountably infinite states to optimally predict.*

Proof This follows as a corollary of Sect. 5's structural propositions—specifically Props. 2 and 3 and Sect. 5.7's conjecture—though translated into the information metrics of Sect. 6.

As discussed above and extensively in Refs. [10–12, 43], nonunifilar HMCs lead to causal state sets of uncountably infinite cardinality and divergent statistical complexity. As the preceding demonstrated, measured quantum processes have presentations that fall into this class.

8 Applications

Having laid out the progression from quantum sources to quantum state processes and their presentations to measured processes and their metrics, we are now ready to illustrate uses and benefits. The following does these via three applications: measurement choice, alternate measurement protocols, and optimal measurements.

8.1 Measurement Variation and Choice

Equations (6) and (8) directly show that choice of measurement basis changes the observed process. This, in turn, means that process' entropy rate and its MSP's statistical complexity dimension also depend on measurement choice. Fortunately, the changes are well behaved.

Conjecture 2 *Measured process complexity depends piecewise smoothly on both the underlying QSSP and choice of measurement.*

Remark 1 Given the extensive development up to this point, the following refrains from presenting formal proofs. These will appear elsewhere. Nonetheless, it is worthwhile to illustrate how the results can be used to outline a construction that supports observed behavior and is backed by formal proofs in parallel problem settings.

Note that:

Fig. 13 cCQS that generates a quantum process with qubits in quantum states $|0\rangle$ and $|a\rangle = \cos \pi/5|0\rangle + \sin \pi/5|1\rangle$
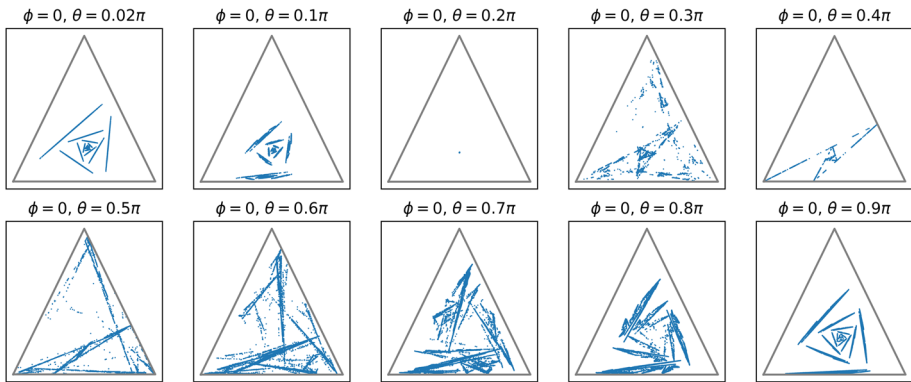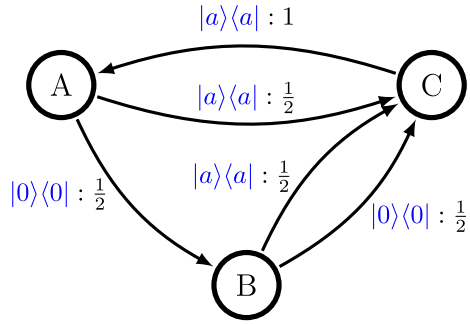

Fig. 14 Mixed-state presentation of the process resulting from measuring the quantum process generated by the cCQS in Fig. 13 in the measurement bases parametrized by (ϕ, θ), as indicated in each subfigure. For each value of the parameters 30,000 mixed states are plotted

1. The measured process' entropy rate and statistical complexity dimension depend smoothly on its MSP's invariant measure, as can be seen from Eqs. (14) and (16).
2. Equations (6) and (8) state that the parameters (transition probabilities) of the measured cCQS HMC depend smoothly on the underlying QSSP and measurement operator parameters.

Therefore, if the MSP's invariant measure depends smoothly on the parameters of the measured cCQS HMC, then the entropy rate and statistical complexity dimension of the measured process depend smoothly on the underlying QSSP and measurement parameters.

Smoothness dependence of the MSP's invariant measure with respect to HMC parameters is not only consistent with observation, which is illustrated shortly, but has been established for many classes of *iterated function system* (IFS). For more detail, Ref. [10] outlines how any HMC can be cast as an IFS—a stochastic dynamical system with a unique attractor (equivalent to an HMC's MSP) that has an invariant measure. Both the attractor and the invariant measure vary smoothly as a function of IFS parameters under contractivity conditions [46–48]. These conditions are generally satisfied by HMCs, thus indicating that both the MSP and invariant measure of an HMC depend smoothly on the HMC parameters. The caveat of piecewise smoothness as opposed to smoothness stems from the fact that the MSP can have abrupt jumps in cardinality for a finite set of parameters, potentially causing finite discontinuities in the statistical complexity dimension, as will be illustrated in the examples of the following section.
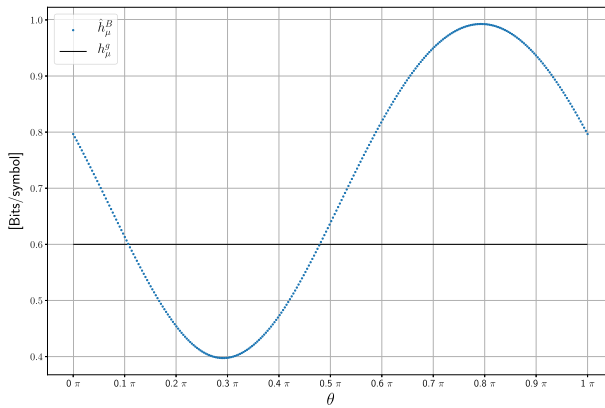
Fig. 15 Entropy rate of the measured cCQSs resulting from measuring the quantum process generated by the cCQS of Fig. 13 as a function of measurement angle θ, as in Eq. (6) at 300 θ values with the value $\phi = 0$ fixed. Entropy rate h_μ^g (black line) of the cCQS that generates the measured process

Beyond smooth dependence, we ask more specifically, How do the mixed-state invariant measure and the associated complexity measures change as a function of the measurement angles θ and ϕ? To answer these questions, we explore two specific examples. For each we choose a quantum process generated by a particular cCQS. We then obtain the measured cCQSs resulting from measuring the quantum process with bases in which one of the angles is held fixed and the other sweeps across its range of possible values.

The two example processes here were chosen since together they illustrate the general properties of measurement dependence of QSSPs. The first example is the three-hidden-state cCQS depicted in Fig. 13, which is then measured in many different qubit bases, holding $\phi = 0$ and varying θ. The second example is the two-hidden-state quantum process generated by the cCQS in Fig. 6, which is then measured following the same procedure.

8.1.1 Random Insertion Process

First, we track changes in the invariant measure on the mixed-state simplex. Figure 14 shows these for the measured process generated by the cCQS of Fig. 13 in 10 different measurement bases (ϕ, θ), as noted there. The structure of the invariant sets $\mathcal{R}$ varies substantially with measurement basis. For most (but one, discussed below) measurement bases the set has an uncountable infinity of states, yet these states have distinct structures that vary smoothly with choice of measurement basis.

Second, we determine the entropy rate as a function of measurement basis in Fig. 15. The process is measured in 300 different bases, holding the value of $\phi = 0$ and varying $\theta \in [0, \pi]$. By comparing to the entropy rate h_μ^g of the cCQS that generates the underlying QSSP, Fig. 15 clearly demonstrates that measurement both increases and decreases the randomness (h_μ).

While this example serves to graphically illustrate the high complexity of predicting the classical stochastic processes measured from the QSSP, there are limitations to estimating the MSP's statistical complexity dimension. For reasons explained in detail in Ref. [11], estimating the statistical complexity dimension for measured cCQSs with MSPs in two and higher dimension simplices is computationally intensive and there is as yet no efficient algorithm. To illustrate the behavior of the statistical complexity dimension in these stochastic
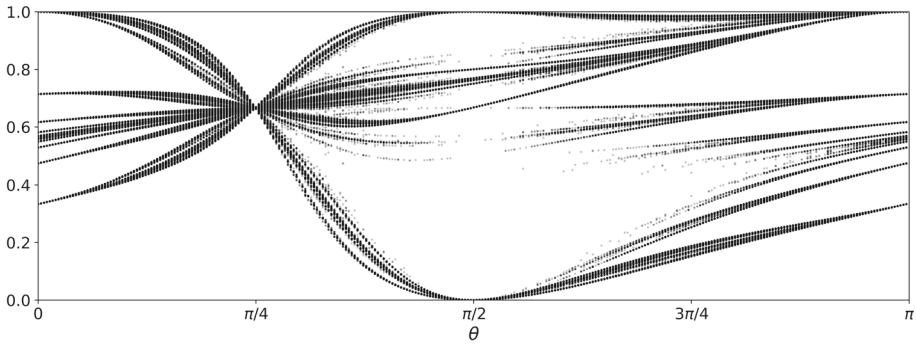
Fig. 16 Mixed-state presentations of the processes resulting from measuring the quantum process generated by the cCQS in Fig. 6 in the bases parametrized by $(\phi = 0, \theta)$. Each vertical line represents the 1D simplex $\mathcal{R}$ and the points in it are the mixed states corresponding to the measured cCQS at that particular value of θ
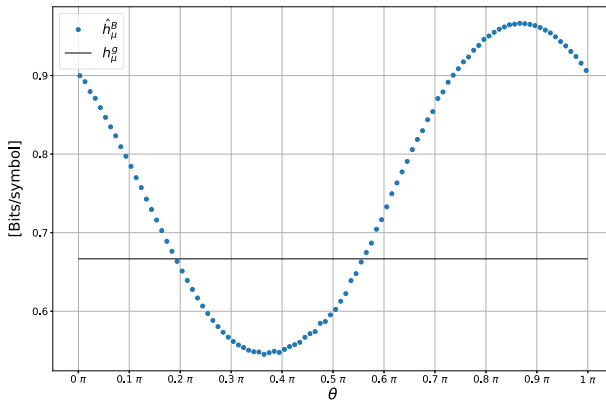

Fig. 17 Entropy rate of the measured cCQSs resulting from measuring the quantum process generated by the cCQS of Fig. 6 as a function of measurement angle θ, as in Eq. (6) with the value $\phi = 0$ fixed, at 100 θ values. Entropy rate h_μ^g (black line) of the cCQS that generates the underlying QSSP

processes, though, we turn to an example of a QSSP generated by a two-state cCQS with an MSP in the 1-simplex.

8.1.2 Golden Mean Process

This example analyzes the QSSP generated by the cCQS in Fig. 6. It is measured in different qubit bases holding $\phi = 0$ fixed and varying θ uniformly from 0 to π. Each measurement yields a measured cCQS that is nonunifilar, the MSP is then computed. Figure 16 displays its invariant measures. Each vertical unit interval corresponds to a 1-simplex that shows the MSP at that particular value of θ. From the figure we observe that the majority of the MSPs have a complex fractal-like structure. However, what the figure makes evident is that this structure varies smoothly with respect to the measurement parameter θ, consistent with Sect. 8.1's Conjecture.

Figures 17 and 18 track how both entropy rate h_μ and statistical complexity dimension d_μ vary with respect to measurement basis.
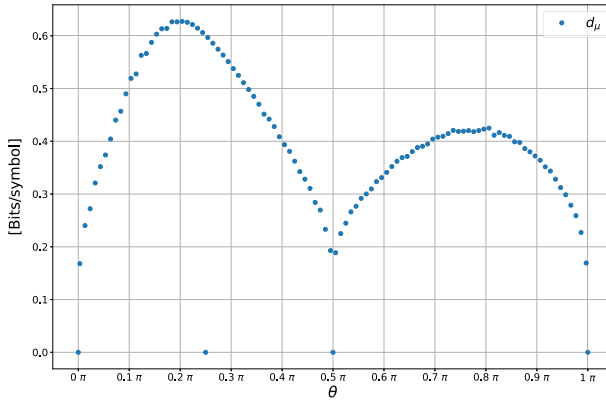
Fig. 18 Statistical complexity dimension d_μ of the measured cCQSs resulting from measuring the quantum process generated by the cCQS of Fig. 6 as a function of measurement angle θ, as in Eq. (6) with the value $\phi = 0$ fixed, at 100 θ values

As with the previous example, we see that h_μ of the measured process both increases and decreases with respect to h_μ^g—that of the original QSSP—depending on measurement basis.

The statistical complexity diverges for most, in contrast with the finite statistical complexity of the underlying QSSP. That said, the statistical complexity dimension d_μ smoothly varies. To a certain extent this reflects what is see from the MSPs in Fig. 16. Figure 18 also reveals four values of θ for which $d_\mu = 0$. These are are $\theta \in \{0, \pi/4, \pi/2, \pi\}$. When θ takes the values 0 or π the measurement is in the observation basis and one of the measurement operators aligns with the quantum state $|0\rangle$. This simplifies the process and thus the measured cCQS has a countably infinite number of mixed states. This also happens at the value of $\theta = \pi/2$, in which one of the measurement operators aligns with the quantum state $|+\rangle$ that is output by the cCQS. Notice that in these three cases, $d_\mu = 0$ is reached smoothly.

The exception to smoothness is the discontinuous jump to $d_\mu = 0$ when the process is measured at $\theta = \pi/4$. This special case is discussed more, shortly. In general terms, though, for that particular basis the measurement does not distinguish between the two distinct emitted qubit states $|0\rangle$ and $|+\rangle$. And so, all of the structural information about the underlying quantum process is lost, except for the probability of obtaining one measurement outcome or the other. The process becomes memoryless and so has a single-state presentation.

8.1.3 General Features

With the previous two examples in hand, and after an exhaustive exploration of example processes in this fashion, we review several common characteristics. Of particular interest are the smooth behaviors of h_μ and d_μ with well defined maxima and minima. It is also apparent that the MSP invariant sets exhibit marked structural variations. However, in agreement with Sect. 8.1's Conjecture, they appear to vary smoothly with respect to measurement change.

A feature that immediately warrants attention in Fig. 14 is the drop in structural complexity of the MSP at $\theta = \pi/5$. With that particular measurement basis, the statistical complexity dimension vanishes, indicating that the measured cCQS is finite. On closer inspection, the HMC corresponding to the measured cCQS is not only finite, but has a single causal state. This indicates that the measured process consists of independent identically distributed (i.i.d.)

random variables. At each time step, the observed symbols are 0 with probability $p_0 = \cos^2 \pi/5$ and 1 with probability $p_1 = \sin^2 \pi/5$. This seemingly special case is not a fluke.

Proposition 5 (Memoryless measurements) *For any cCQS with quantum alphabet $\mathcal{A}_Q$ consisting of two distinct quantum states ρ_a and ρ_b, there exists a set of measurement bases for which the resulting measured process is memoryless and $C_\mu = 0$.*

Proof We establish this by construction. Without loss of generality and for ease of notation we align both quantum states with the zx-plane, such that one of the quantum states ρ_a is at the top of the Bloch sphere. We further denote the angle between the two states by α. We then write $\rho_a = |0\rangle\langle 0|$, and $\rho_b = |b\rangle\langle b|$ such that $|b\rangle = \cos \alpha/2 |0\rangle + \sin \alpha/2 |1\rangle$.

Consider the projective measurement bases for which one measurement operator projects onto a state $|\psi_0\rangle$, such that $|\langle\psi_0|0\rangle| = |\langle\psi_0|b\rangle|$. That is, $|\psi_0\rangle$ lies in the Bloch sphere circumference that bisects the angle between $|0\rangle$ and $|b\rangle$. Then, the set of measurements that project onto $|\psi_0\rangle$ and $|\psi_0^\perp\rangle \equiv |\psi_1\rangle$ are such that the probability distributions over measurement outcomes are the same whether the measured qubit state was ρ_a or ρ_b. That is, for this particular set of measurements, we have $\Pr(i|\rho_j) = p_i$ for $i \in \{0, 1\}$ and for all ρ_j with p_i a constant and $p_0 + p_1 = 1$.

Together with Eq. (8), this observation says that the measured cCQS transition matrices are, for $i \in \{0, 1\}$:

$$
\begin{aligned}
T^i &= \mathbb{T}^{\rho_a} Pr(i|\rho_a) + \mathbb{T}^{\rho_b} Pr(i|\rho_b) \\
&= p_i (\mathbb{T}^{\rho_a} + \mathbb{T}^{\rho_b}) \\
&= p_i \mathbb{T} \ .
\end{aligned}
\tag{17}
$$

That is, both labeled transition matrices are proportional to each other and to $\mathbb{T}$. Note also that $T = T^0 + T^1 = \mathbb{T}$, so for simplicity we refer to the internal Markov chain transition matrix as T.

Both labeled transition matrices being proportional to T implies that the MSP yields a biased coin process with biases p_0 and p_1, respectively. There is a single recurrent mixed state, namely π. This follows by definition, since π is an eigenvector of T. And so, evolving the mixed state $\eta_t = \pi$ gives:

$$
\begin{aligned}
\eta_{t+1} &= \frac{\pi \cdot T^i}{p_i} \\
&= \pi \cdot T \\
&= \pi \ .
\end{aligned}
$$

Physically, memoryless measurements project states onto a basis whose components are symmetric with respect to the pure states in $\mathcal{A}_Q$. Consequently, the measurement cannot distinguish between the pure states and so the act of measurement effectively leads to a complete loss of information about the cCQS's internal structure.

The fact that these memoryless measurements maximize the loss of information about the cCQS's internal structure, naturally leads to the question of whether there exists a set of measurements that maximally preserves information about the cCQS's internal structure. These would be measurements that optimally distinguish between the quantum states. In the case of POVMs these measurements are well studied for the case of distinguishing between 2 or 3 states. And, as explored in Sect. 8.2.1 they in fact yield special measured processes.

Shortly, we return to explore the issue of optimal and extremizing measurement bases.

Another point to make is that in all of the examples above, only the θ parameter of the measurement bases was varied, and the phase ϕ was fixed to zero. This choice was for simplicity and visualization purposes only. The variation of ϕ does not change the analysis or the conclusions in any way. The only notable point is that when the measurement parameters both define a measurement basis that is not close to being aligned with any of the output quantum states and is poor at distinguishing between them, then that will in general result in processes that have h_μ larger than the underlying cCQS and, as is generally the case, divergent memory.

Appendix F graphically demonstrates this with two animations that sweep the angles θ and ϕ while monitoring entropy rate and mixed states. One animation shows how the mixed state presentation and h_μ vary a function of parameter θ. The other animation shows $h_\mu(\theta)$ plots as in Fig. 15 while sweeping ϕ from 0 to 2π.

In general, as seen from Fig. 15, different choices of measurement increase or decrease the randomness of the measured quantum process. Furthermore, even if the general case is that quantum measurement dramatically increases the structural complexity of the measured stochastic process with respect to the underlying quantum process, the existence of memoryless measurements shows that particular choices of measurement, in fact, can mask the quantum process' structural complexity.

8.2 Alternate Measurement Protocols

While simplicity dictated that the preceding concentrate on protocols in which the same projective measurement is applied at every time step, there are many alternative protocols to explore. As an example, the following considers processes that result from applying more general measurements to each emitted qubit.

8.2.1 Positive Operator-Valued Measurements

The development to this point investigated the consequences for the observed classical stochastic process of employing only projective measurements. However, the natural generalization is to more flexible positive operator-valued measurements.

Definition 12 (*Positive Operator-Valued Measurement on a QSSP*) A *positive operator-valued measurement* (POVM) $\mathcal{I}$, consists of a finite set of positive semi-definite operators $\{E_x\}$, on the Hilbert space $\mathcal{H}^d$ of dimension d. The operators satisfy the condition $\sum_x E_x = \mathbb{I}_d$. When measurement $\mathcal{I}$ acts on a quantum system in state ρ_t, emitted by a QSSP, the outcome is x_t, corresponding to operator E_x, with probability:

$$\Pr(x_t|\rho_t) = tr(\rho_t E_{x_t})$$

Applying a POVM to every quantum state emitted by the QSSP yields a classical stochastic process over the values of $x \in \mathcal{A}_M$—the alphabet of the measured process.

When the measurement $\mathcal{I}$ consists of a POVM, the number of operators $\{E_j\}$ and possible outcomes can be any positive integer. This increase in possible measurement outcomes results in a larger alphabet for the classical measured quantum process. At first glance, this suggests finding a wider range of unifilar measured HMCs, but it is not. This is a direct result of indistinguishability.

Generally, when performing a POVM on any two qubit states (even distinguishable ones), at least one of the measurement outcomes has a nonzero probability of being observed on
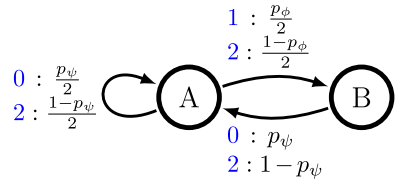
both of the quantum states. This is due to the fact that POVMs generally have nonorthogonal measurement operators.

When measuring with a POVM, consider a cCQS hidden state with two outgoing transitions on distinct quantum states. Applying the POVM on those transitions means that at least one of the symbols in the classical alphabet $\mathcal{A}_M$ is present in two outgoing transitions for the same hidden state in the measured cCQS. This makes the dynamic of the measured cCQS nonunifilar. Thus, in general when using POVMs, measured processes are also highly complex, akin to those obtained when applying projective measurements.

That said, the measured processes produced using POVMs reveal a new collection of notable special cases, which remain to be broadly explored. To illustrate just one, the following develops a simple but illuminating example using the unambiguous state discrimination POVM. The resulting flexibility then leads, in the following section, into the challenge of optimizing measurement protocols to achieve various ends.

8.2.2 Unambiguous State Discrimination

Recall that when measuring qubits either in state $|\psi\rangle$ or $|\phi\rangle$, the POVM yielding the highest probability of unambiguously distinguishing between them is given by [49–51]:

$$E_\psi = \frac{1}{1 + |\langle\phi|\psi\rangle|}|\phi^\perp\rangle\langle\phi^\perp| \tag{18a}$$

$$E_\phi = \frac{1}{1 + |\langle\phi|\psi\rangle|}|\psi^\perp\rangle\langle\psi^\perp| \tag{18b}$$

$$E_? = \mathbb{I} - E_\psi - E_\phi . \tag{18c}$$

Applying this measurement scheme to the quantum process generated by the cCQS in Fig. 3 produces the classical process emitted by the HMC of Fig. 19. There $\{E_\psi, E_\phi, E_?\}$ are relabeled $\{E_0, E_1, E_2\}$, $p_\psi = \text{Tr}(E_0|\psi\rangle\langle\psi|)$, and $p_\phi = \text{Tr}(E_1|\phi\rangle\langle\phi|)$.

Note that symbol 2, corresponding to an inconclusive measurement, is present in all transitions. Yet observing 0 or 1 is synchronizing since they each determine the next HMC state. This property is preserved from the cCQS that is being measured and need not occur generally. That said, if the cCQS under study outputs only two distinct quantum states, then measuring it with the unambiguous state discrimination POVM in Eq. (18) results in an HMC presentation that preserves the internal topology. However, each HMC transition is corrupted with a nonzero probability of observing symbol 2, rendering an inconclusive measurement.

For this example, constructing the MSP for the process generated the cCQS in Fig. 19 produces the presentation depicted in Fig. 20, where transition probabilities are not shown to reduce clutter.

There is a subset of MSP states with topology similar to the original cCQS, but augmented with the mixed states that capture the observation of 2s. This generally holds when the
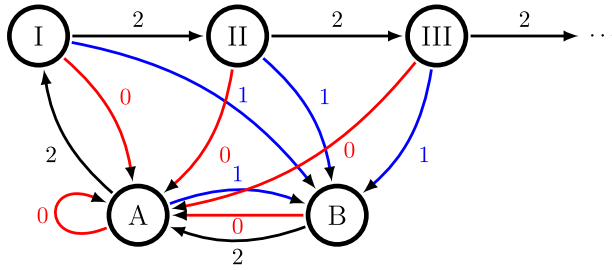
Fig. 20 State transition diagram of the MSP constructed from the HMC in Fig. 19. Transition probabilities omitted for clarity. Observing 1s (blue transitions) leads to state *B*; observing 0s (red transitions) to state *A*. Both cases are synchronizing

generator is a unifilar cCQS that emits two distinct nonorthogonal quantum states if the process is measured via the POVM in Eqs. (18). In the measured cCQS, there will be a subset of MSP states that mimic the cCQS's internal dynamics, but the latter is augmented by inconclusive measurement outcomes. And, there are chains of mixed states that drive the process away from the original dynamic whenever a sequence of "inconclusive results" or a nonsynchronizing symbol is observed.

To explore this process further set:

$$|\phi\rangle = |0\rangle$$
$$|\psi\rangle = \cos{(\alpha/2)}|0\rangle + \sin{(\alpha/2)}|1\rangle ,$$

with $\alpha \in (0, \pi)$. Then, $p_\psi = p_\phi = 1 - \cos{(\alpha/2)}$. When constructing the MSP of Fig. 20, all transitions that emit a 2 (black) have an associated probability of $\cos{(\alpha/2)}$, while the probabilities of the blue and red transitions depend on the specific transition. As the number of 2s observed approaches infinity, the mixed states visited approach the stationary state distribution $\pi = (2/3, 1/3)$ of the nonunifilar measured cCQS.

This MSP, while requiring a countable infinity of states, is so well behaved that it allows for direct calculation of the mixed states and the numerical computation of both its entropy rate and statistical complexity by approximating the MSP with a finite but sufficiently large set of mixed states. Figure 21 plots both the entropy rate and statistical complexity when the processes are approximated by a MSP with 500 hidden states.

Figure 21 reveals edge cases that match expectations. At one extreme, when $\alpha = 0$, the process reduces to a sequence of qubits in state $|0\rangle$. Thus, both process randomness and structure vanish. At the other extreme, when $\alpha = \pi$, the alphabet emitted by the cCQS is orthogonal $\{|0\rangle, |1\rangle\}$. Hence, the unambiguous state discrimination POVM reduces to the projective measurement aligned with the observation basis. This means that the measured process is true to the original quantum source and both its entropy rate and statistical complexity coincide with h_μ^g and C_μ^g, respectively. The plots also highlight that both entropy rate and statistical complexity coincide with the generator values with different nonorthogonal alphabets and that their maximum values are attained for different alphabets as well. While both randomness and structure of the measured process depend on the cCQS's quantum alphabet, they both have distinct meanings and, thus, the dependencies are not equivalent.

When varying the quantum alphabets and exploring α's whole range, it becomes apparent that the values of both entropy rate and statistical complexity can be lower or higher than those of the original cCQS. This means that for a given cCQS and a given measurement both the randomness and structure of the measured process with respect to the QSSP can be
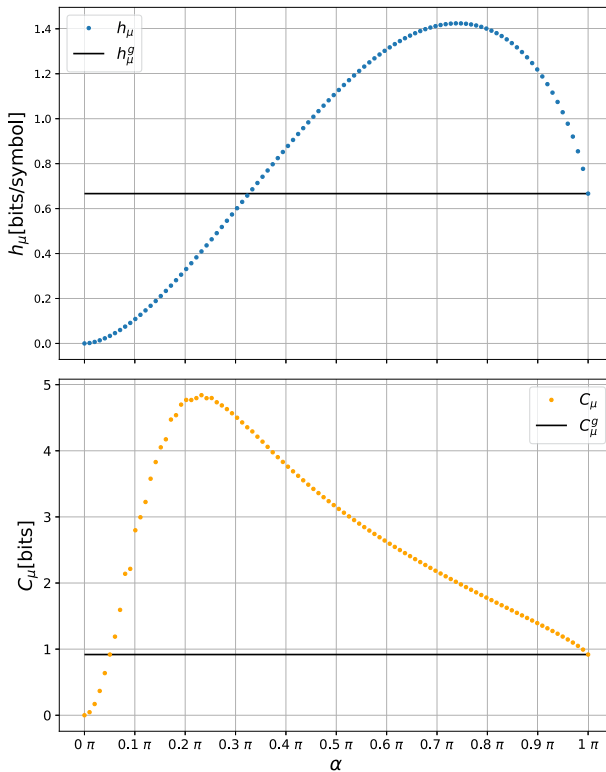
Fig. 21 (Top) Randomness h_μ and (bottom) statistical complexity C_μ as a function of the angle α between the two states emitted by the cCQS in Fig. 3, with $|\phi\rangle = |0\rangle$ and $|\psi\rangle = \cos(\alpha/2)|0\rangle + \sin(\alpha/2)|1\rangle$. The horizontal black lines show the values of h_μ^g and C_μ^g of the cCQS that generates the original quantum state process

reduced or increased. This makes plain the possibly ambiguous effects of measurement and what the latter can add to or remove from the underlying quantum process.

Figure 22's *complexity-entropy diagram* [52] offers a more concise display of the QSSP's achievable information generation and storage—its *intrinsic computation*—when measured in this particular POVM across the range of alphabets. Notice that for small h_μ the system's structure or memory requirements C_μ are low. Then memory increases with increased randomness until a peak is reached at about $h_\mu = 0.4$ bits/symbol. Above this, increased randomness requires fewer memory resources and a given randomness can be achieved at more than one memory value C_μ.

Overall, this example illustrates a situation in which a particular choice of measurement protocol leads to a very tractable measured process. While the statistical complexity diverges for most measured processes, this example shows that tailoring measurement schemes still leads to complex, but more tractable dynamics. That is, the observed dynamics can be leveraged to better understand the dynamic that produces the underlying QSSP.

9 Optimal Measurements

The previous sections established the two main characters of measured quantum processes—their unpredictability and temporal correlation. And, they demonstrated how measurement
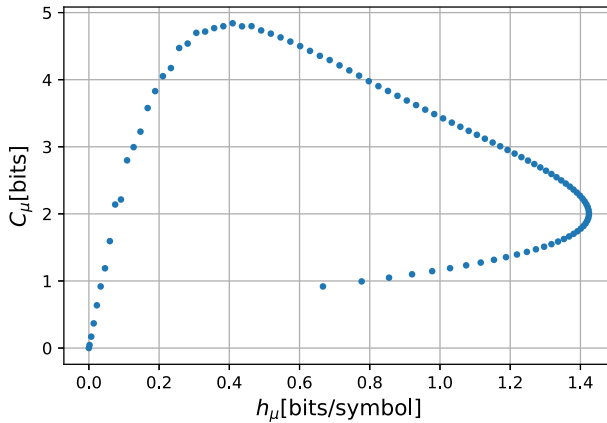
Fig. 22 Complexity-entropy diagram capturing the purely informational character of the measured quantum-state process: Parametric plot of $h_\mu(\alpha)$ and $C_\mu(\alpha)$ over $\alpha \in [0, \pi]$ illustrating how the intrinsic informational properties depend on each other without reference to model parameter α. Cf. complexity-entropy plots in Ref. [52]

can increase or decrease observed randomness and structure. These metrics naturally broach the challenge of defining and demonstrating the existence of informationally-optimal measurements. The possibility of these optimizations is greatly facilitated by the piecewise smooth dependence of the informational metrics on the QSSP and on measurement operators.

Eschewing details, the following lays out several avenues for future exploration, illustrating various kinds of optimality using the tools now in hand. We consider, in turn, measurements that lead to minimal structural complexity and to various forms of maximal informativeness. The following cases only address projective measurements, though extension to POVMs is in some cases straightforward and of interest in general.

Developing algorithms and calculational methods to find and implement these optimal measurements is left to the future.

Let's briefly recall relevant notation. A given projective measurement protocol is denoted $\mathcal{E}$. Given a QSSP $R_{-\infty:\infty}$ and a measurement protocol $\mathcal{E}$, the corresponding measured process is $X_{-\infty:\infty} = \mathcal{E}(R_{-\infty:\infty})$. To simplify the notation the following introduces $\mathcal{E}(M)$—the MSP of the measured cCQS of $X_{-\infty:\infty}$ for a given cCQS M.

The following treats the alternative informational metrics as operators themselves. So that for HMC M, $h_\mu(M)$ is that HMC's entropy rate, $C_\mu(M)$ is its statistical complexity, and $d_\mu(M)$ its statistical complexity dimension.

9.1 Minimal Structural Complexity

There are settings where it is useful to identify and use measurements that lead to the least complex, smallest-memory observed process. Such measurement schemes are specified as follows.

Definition 13 (*Minimal Structural Complexity Measurement*) Given a cCQS M, the projective measurement $\mathcal{E}_{C_\mu}$ that leads to the measured process with the minimal structural complexity is, when $\mathcal{E}(\overline{M})$ is finite state:

$$\mathcal{E}_{C_\mu} = \underset{\{\mathcal{E}\}}{\arg\min}\, C_\mu(\mathcal{E}(M))$$

and when $\mathcal{E}(M)$ uncountably infinite state:

$$\mathcal{E}_{\underline{C_\mu}} = \arg\min_{\{\mathcal{E}\}} d_\mu(\mathcal{E}(M)) \ .$$

While this kind of measurement is the least informative about the underlying quantum dynamics, it has also proven in multiple examples to be the measurement that yields a classical process requiring the least memory resources to simulate and predict. This remains to be proven but is consistent with the fact that the measurement effectively is the most efficient at discarding information about the structure of the underlying process, which need not be stored to represent the resulting measured process.

9.2 Maximally Informative Measurements

Perhaps most naturally, one can employ a measurement scheme that maximizes the amount of information per symbol in the measured process. Such measurement schemes are specified as follows.

Definition 14 (*Maximally Informative Measurement*) Given a cCQS M, the projective measurement $\mathcal{E}_{\overline{h_\mu}}$ that leads to the measured process with maximally informative measurement outcomes is:

$$\mathcal{E}_{\overline{h_\mu}} = \arg\max_{\{\mathcal{E}\}} h_\mu(\mathcal{E}(M)) \ .$$

Recalling basic dynamical systems, this is a natural choice of optimal measurement in that it mimics the essence of what a generating partition is, as defined by Kolmogorov and proven by Sinai [53]. In this case, each observation of a measurement outcome X_t results in the maximum possible amount of new information.

9.3 Maximally Mutually-Informative Measurements

One is often interested in monitoring how measurement outcomes reveal (or not) the internal generating mechanism. This suggests the following measurement.

Definition 15 (*Maximally Mutually-Informative Measurement*) Given a QSSP $R_{-\infty:\infty}$, the measurement protocol $\mathcal{E}_{\overline{R:X}}$ is *the maximally mutually informative measurement* when:

$$\mathcal{E}_{\overline{R:X}} = \arg\max_{\{\mathcal{E}\}} I(R_{-\infty:\infty} : X_{-\infty:\infty}) \ ,$$

where $I(R_{-\infty:\infty} : X_{-\infty:\infty})$ is the mutual information [54] between the QSSP and the measured process.

This measurement maximizes the information shared between the quantum-state stochastic process and the measured quantum process. That is, observation of the classical process maximally reduces uncertainty of the quantum process. In contrast to the *maximally informative measurement*, the *maximally mutually-informative measurement* does not yield the maximal amount of information learned per observation of the measured process. Rather, it provides the maximal amount of information learned about the QSSP given observation of the measured process.

9.4 Dynamically Informative Measurements

Finally, one may be interested in finding the measurement that yields a stochastic process most similar to the underlying QSSP. This requires adhering to a particular definition of distance or similarity between stochastic processes. One option when working with a particular cCQS and its corresponding measured cCQS is to use a measure of distance between HMCs. The measurement that minimizes the distance between two HMCs is the most informative about the internal structure of the QSSP generated by the cCQS. Said simply, it is the measurement yielding a classical stochastic process that is most informative about the QSSP's dynamical structure.

Selecting an appropriate measure of distance between HMCs is not a straightforward problem. Many have been proposed [55–57], each with their own nuances. Determining which distance measure better suits the problem at hand is left for future work.

This and the above notions of optimality are distinct and so are of interest in different operational settings. It is important to emphasize that, what differentiates these optimality criteria from other notions of measurement optimality is that they depend on the QSSP's time correlations and not only on the particular quantum state of a single quantum system or its evolution.

10 Conclusion

To investigate temporal complexity—unpredictability and structure—in quantum dynamics we developed an intentionally simplified setting—one that excluded sequential qubit entanglement. This allowed deploying classical multivariate information theory as a quantitative analysis tool. And, this led directly to isolating the problem of how measurement affects the appearance of quantum processes—processes to which one must apply a quantum measurement to observe. The simple lesson is that measurement can both increase or decrease randomness and structure. In point of fact, and somewhat unanticipated, observing a quantum process through projective measurements results in an observed classical process of explosively high structural complexity. The detailed analysis enriched this by identifying the mechanisms through which this complexity arises.

In general, quantum-state stochastic processes observed through projective measurements result in observed classical processes that require storing an infinite number of predictive features to allow for optimal prediction. The sets of predictive features for most processes are rich in structure and, making use of that, we implemented newly developed tools to quantify their structural complexity and the intrinsic randomness of the measured process. In addition, the development shed light on the influence that the chosen measurement basis has on the complexity of the observed process.

Irreducible nonunifilarity was identified as the driving mechanism of these features. The low dimensionality of the quantum state Hilbert space is the physical cause. Nonalignment between the measurement basis and emitted quantum states of the cCQS is the root physical mechanism that leads to induced indistinguishability of quantum states.

Even allowing for the framework's simplifications, the typical complexity of the measured process complicates not only its study, but also makes the task of learning about the underlying quantum process a difficult one. We made progress in understanding why that is and how to characterize the measured processes. That progress came from adapting new methods from

ergodic theory and random dynamical systems to this setting. The result is a powerful toolset for quantitatively analyzing measured quantum processes.

We showed that the underlying cCQSs have distinct signatures of structure and randomness as a function of the measurement parameters and that dependence is systematic and smooth. One remaining task is to characterize the possible underlying quantum sources that generate a given measured cCQS or, at the very least, their statistical properties.

In this way, the results lay a path to fully characterizing quantum state stochastic processes. However, many steps remain unexplored. We conjecture that success in these will have broad impacts. One of those steps is to find the spectral decompositions of the processes by use of meromorphic functional calculus [58]. While these tools are not engaged here, they will be necessary when studying CQSs generated by purely quantum controllers. Another essential step is to model the internal controller in such a way that it generates entangled QSSPs. There are helpful starting points for this in both finite-memory classical controllers [59] and quantum protocols [60, 61] for sequential generation of matrix product states. The latter are of particular interest in the study of many-body entangled states.

We only briefly explored a measurement protocol that used single qubit POVM measurements. This showed that exploring different measurement protocols has the potential to bring novel results and to move closer to more physically realistic settings. For example, Ref. [38] looks at measurements that allow synchronization to the underlying QSSP in a setting similar to that explored here. As in the study of classical dynamical systems, though, understanding the informational and statistical effects of choosing a particular measurement instrument or protocol can aid in optimizing particular tasks. The study of optimal quantum measurements for QSSPs remains as a challenging open problem.

A major challenge is to extend the current setting to quantally-controlled qubit sources (qCQS), as just noted. And, then, from there to develop a quantum communication channel setting in which qubits are input, quantally processed, and then output. Advances in this will more directly impact information processing and computing performed by quantum dynamical systems. Beyond that, qubit source timing issues should be addressed, moving away from the admittedly simple use of discrete time here to continuous-time processes. Fortunately, the cCQS model can easily be extended to discrete-event continuous-time hidden semi-Markov models using the methods of Ref. [62]. This will immediately give metrics of quantum randomness and structure, paralleling the development here.

Extending the present results along these lines will naturally complement existing quantum descriptions of classical stochastic processes [63–65]. They also flag a starting point from which to understand the statistical and structural properties of quantum-state time series. That step will provide tools necessary not only for furthering our understanding of fundamental quantum dynamics, but also grasping the operational meaning of their informational properties in the context of quantum computation.

Declarations

Appendix A: Stochastic Processes

The Appendices provide a summary of and an introduction to the classical theory that is the foundation for the main development. They cover basic notation and definitions, as well as hidden Markov chains and their properties and uses that are most relevant.

A classical stochastic process $\mathbf{X}$ is a bi-infinite series of indexed observables produced by a system and is defined by the probability measure over the random variables corresponding to the observables: $\Pr\left(\ldots X_{t-1}, X_t, X_{t+1}\ldots = \ldots x_{t-1}, x_t, x_{t+1}\ldots\right)$. In this, the random variables corresponding to the observables are denoted with capital letters $\ldots X_{t-2}, X_{t-1}, X_t, X_{t+1}, X_{t+2}\ldots$ and their realizations are denoted by lowercase letters $\ldots x_{t-2}, x_{t-1}, x_t, x_{t+1}, x_{t+2}\ldots$, with the x_t values drawn from a discrete alphabet $\mathcal{A}$. The label t in the indexing is chosen to evoke the traditional time-indexing of stochastic processes in which the random variables are sequential measurements of a physical system. Random variable blocks are denoted $X_{t:t+l} = X_t, X_{t+1}, \ldots X_{t+l-1}$, with the left index inclusive and the right exclusive.

For present purposes, we concentrate on *stationary* stochastic processes, in which the joint distribution for a block of length l is time (or index)-translation invariant:

$$\Pr\left(X_{t:t+l} = x_{t:t+l}\right) = \Pr\left(X_{0:l} = x_{0:l}\right) ,$$

for all t and l. A wide class of stationary stochastic processes can be modeled with Hidden Markov Chains (HMCs) [32, 33, 42]. Appendix C describes these in detail, reviewing how they facilitate calculating various metrics for the stochastic processes they generate.

Appendix B: Process Markovity

Given that the present setting considers both classical stochastic process theory and quantum phenomena, it is helpful to comment on the concept of Markovianity.

Definition 16 A *Markov process* or *Markov chain* of order R is a stationary stochastic process $\mathbf{X}$ in which the probability distribution satisfies the following:

$$\begin{aligned}
&\Pr\left(X_t = x_t | X_{-\infty:t} = x_{-\infty:t}\right) \\
&= \Pr\left(X_t = x_t | X_{t-R:t} = x_{t-R:t}\right) \\
&= \Pr\left(X_t = x_t | X_{t-1} = x_{t-1}\ldots X_{t-R} = x_{t-R}\right),
\end{aligned} \tag{19}$$

for all $t \in \mathbb{Z}$ and $R \in \mathbb{N}$.

That is, the probability distribution of a particular random variable conditioned on the past depends only on the value of the previous R random variables.

From this definition, we emphasize the following:

- Memoryless or independent identically distributed (*i.i.d.*) processes are stochastic processes with $R = 0$. We also refer to them as Markov processes of order 0.
- Stochastic processes with $1 \leq R < \infty$ are memoryful. We refer to them as Markov processes of order R.
- Memoryful stochastic processes that do not satisfy the Markov condition in Eq. (19) for finite R, but require $R = \infty$ are infinite-order Markov processes. The latter is a surprisingly common property [66]. They are the best candidates for the descriptor "non-Markov processes".

These points are necessary as there is contradictory use of the terminology in the quantum non-Markovianity literature. In particular, there is extensive use of the descriptor "memoryless" to refer to Markov processes with Markov order $R = 1$ and "non-Markovian" to refer to processes with finite Markov order $R > 1$ [6, 23, 27, 67, 68]. While those use cases are in dynamical settings distinct from the one we address here it is pertinent to clarify our nomenclature.

To avoid confusion, the nomenclature above is directly derived from the definition of the Markov property, consistent with A. A. Markov's original motivations to study "complex chains", his phrase for memoryful stochastic processes [24, 25, 69, 70]. Memoryless is $R = 0$, Markov is $1 \leq R < \infty$, and infinite Markov or non-Markov is $R = \infty$. Reference [71]'s introduction reviews this and the early history of probabilistic chains.

Appendix C: Hidden Markov Chains

Definition 17 A *hidden Markov chain* (HMC) is a tuple $(\mathcal{S}, \mathcal{A}, \{T^x\})$ that consists of:

- Set $\mathcal{S}$ of hidden states $\sigma \in \mathcal{S}$.
- Discrete alphabet $\mathcal{A}$: a set of symbols that the HMC emits on state-to-state transitions at each time step.
- $\{T^{(x)}\}$, $x \in \mathcal{A}$ is the set of symbol-labeled transition matrices such that $T^{(x)}_{\sigma\sigma'} = Pr\left(x, \sigma'|\sigma\right)$ with $\sigma, \sigma' \in \mathcal{S}$.

The tuple directly defines the dynamic over the hidden states, which is itself Markovian (order $R = 1$). That Markov chain's transition matrix is given by $T = \sum_{x \in \mathcal{A}} T^x$. In turn, T defines the stationary state distribution π over hidden states, such that $\pi \cdot T = \pi$. That is, π is a row vector such that $\pi_\sigma = \Pr(\sigma)$ with $\sigma \in \mathcal{S}$.

See, for example, Fig. 5, where $\mathcal{S} = \{A, B\}$ and $\mathcal{A} = \{0, 1\}$.

An HMC then is a model for a stochastic process consisting of the set of emitted symbol sequences and their associated probabilities. It is important to note here that, even if the dynamic over hidden states is Markovian, HMCs generate a more general class of stochastic processes that includes non-Markovian processes. While the hidden states give an explicit mechanism for producing a stochastic process, the stochastic process itself is defined only over the set of symbols $x \in \mathcal{A}$.

HMCs are useful in that they specify a finite mechanistic procedure to produce the correct probabilities for a stochastic process. There is an infinite family of distinct HMCs that model a given process. These are called a process' *presentations*. For each process, though, there is a unique presentation with specific properties that, beyond merely generating the correct

probabilities, captures the minimal conditional distributions needed for optimal prediction. This presentation is called a process' ϵ-machine, and it allows for efficient exact computation of a process' randomness and structure metrics. Appendix D summarizes what an ϵ-machine is and why it is such an important tool when modeling a stochastic process.

In point of fact, the development here works with *edge-labeled* HMCs. There are also *state-labeled* HMCs that emit symbols on entering a state. Both presentation classes generate the same class of stochastic processes. They are equivalent in this sense and they can be directly interconverted. Edge-labeled presentations, though, do offer computational advantages when calculating informational properties and in interpreting the functionality of their operation.

Appendix D: Computational Mechanics

This section briefly reviews the main results of *computational mechanics* [13–15].

For ease of notation, we refer here to the past sequences of a process as $\overleftarrow{X} = X_{-\infty:t}$ and the future sequences as $\overrightarrow{X} = X_{t:\infty}$. For finite futures of length ℓ we use $X_{t:t+\ell} = \overrightarrow{X}^{\ell}$.

As addressed in the main text, the hidden states in a unifilar presentation must satisfy the condition that, given an observed past sequence $\overleftarrow{x}$, all the allowed hidden states induced by that observation must have the same distribution of futures $\Pr\left(\overrightarrow{X} \mid \overleftarrow{x}\right)$. If every observed past induces a unique allowed state in a unifilar presentation, we call that a *causal state*.

Definition 18 *Causal states* are the equivalence classes of pasts determined by the equivalence relation $\sim_{\epsilon}$. The latter defines two infinite past sequences $\overleftarrow{x}$ and $\overleftarrow{x}'$ as equivalent—$\overleftarrow{x} \sim_{\epsilon} \overleftarrow{x}'$—if and only if they have the same conditional distribution of futures:

$$\epsilon(\overleftarrow{x}) = \left\{ \overleftarrow{x}' \mid \Pr\left(\overrightarrow{X}^{\ell} = \overrightarrow{x}^{\ell} \mid \overleftarrow{X} = \overleftarrow{x}\right) = \Pr\left(\overrightarrow{X}^{\ell} = \overrightarrow{x}^{\ell} \mid \overleftarrow{X} = \overleftarrow{x}'\right) \right\},$$

where $\overrightarrow{x}^{\ell} \in \overrightarrow{X}^{\ell}$, $\overleftarrow{x}' \in \overleftarrow{X}$, and $\ell \in \mathbb{Z}^{+}$. We denote a causal state random variable by $\mathcal{S}$, a particular causal state of an HMC by σ, and the set of causal states by $\boldsymbol{\mathcal{S}}$.

As Ref. [14] details, a given causal state and the next observed symbol of a process determine a unique next causal state. A given causal state σ also provides a well-defined conditional probability $\Pr(\overrightarrow{X} \mid \sigma)$ for all possible future sequences $\overrightarrow{X}$. These two facts together mean there is a well-defined set of labeled transition matrices $\{T^{(x)}\}$ that describe the probabilities of transition between causal states given an observed symbol x.

Definition 19 The causal state set $\boldsymbol{\mathcal{S}}$, together with the labeled transition matrices $\{T^{(x)} : x \in \mathcal{A}\}$ define a process' ϵ-machine.

For any given stochastic process, its ϵ-machine is unique. It is also the process presentation with maximally accurate prediction of minimal statistical complexity. This makes the ϵ-machine a natural canonical HMC for a process.

Appendix E: Mixed-State Presentations

The following introduces the *Mixed State Algorithm* (MSA) that converts a nonunifilar presentation to a unifilar presentation.

Assume that an observer has an HMC presentation M for a process $\mathcal{P}$ that emits symbols $x \in \mathcal{A}$. Before making any observations, it has probabilistic knowledge of the current state

$\eta_0 = \Pr(\mathcal{S})$. We call this a *state of knowledge* or *belief distribution*. Typically, the best guess for an observer prior to observing any output of the system is $\eta_0 = \pi$.

Once M generates a word $w = x_0 x_1 \ldots x_\ell$ the observer's *state of knowledge* of M's current state can be updated to $\eta(w)$, that is:

$$\eta(w)_\sigma \equiv \Pr(\mathcal{S}_\ell = \sigma | X_{0:\ell} = w, \mathcal{S}_0 \sim \pi) . \tag{E1}$$

The collection of possible *states of knowledge* $\eta(w)$ forms M's set $\mathcal{R}$ of *mixed states*:

$$\mathcal{R} = \{\eta(w) : w \in \mathcal{A}^+, \Pr(w) > 0\} ,$$

where $\mathcal{A}^+$ is the set of all words with positive length.

There is also the mixed-state measure $\mu(\eta)$—the probability of being in a particular mixed state:

$$\Pr(\eta(w)) = Pr(\mathcal{S}_\ell | X_{0:\ell} = w, \mathcal{S}_0 \sim \pi) \Pr(w) .$$

From this follows the probability of transitioning from $\eta(w)$ to $\eta(wx)$ on observing symbol x:

$$\Pr(\eta(wx) | \eta(w)) = \Pr(x | \mathcal{S}_\ell \sim \eta(w)) .$$

This defines the mixed-state dynamic $\mathcal{W}$, in terms of the original process not in terms of an HMC presentation of the latter.

Given any presentation M of a process, we can calculate a new presentation for the process with important properties as follows. The probability of generating symbol x when in mixed state η is:

$$\Pr(x | \eta) = \eta \cdot T^{(x)} \cdot \mathbf{1} , \tag{E2}$$

where $\mathbf{1}$ is a column vector of ones. Upon seeing symbol x, the current mixed state η_t is updated:

$$\eta_{t+1}(x) = \frac{\eta_t \cdot T^{(x)}}{\Pr(x | \eta)} . \tag{E3}$$

Thus, given an HMC presentation we calculate the mixed state of Eq. (E1) via:

$$\eta(w) = \frac{\pi \cdot T^{(w)}}{\pi \cdot T^{(w)} \cdot \mathbf{1}} .$$

And the mixed-state transition dynamic is then:

$$\Pr(\eta_{t+1}, x | \eta_t) = \Pr(x | \eta_t)$$
$$= \eta_t \cdot T^{(x)} \cdot \mathbf{1} ,$$

since Eq. (E3) says that, by construction, the MSP is unifilar. That is, the next mixed state is a function of the previous and the emitted (observed) symbol.

Together the mixed states and their dynamic give the HMC's *mixed-state presentation* (MSP) $\mathcal{U} = \{\mathcal{R}, \mathcal{W}\}$, a unifilar presentation for the process generated by presentation M.

Appendix F: Measurement Angle Dependence

Two animations illustrate the measurement angle dependence of the MSP; see: https://csc.ucdavis.edu/~cmg/compmech/pubs/qdic.htm.

The first animation shows shows how the mixed state presentation and h_μ vary as a function of parameter θ. The second animation shows plots like that in Fig. 15, while sweeping ϕ from 0 to 2π.

References

1. Schindler, P., Barreiro, J.T., Monz, T., Nebendahl, V., Nigg, D., Chwalla, M., Hennrich, M., Blatt, R.: Experimental repetitive quantum error correction. Science **332**(6033), 1059 (2011)
2. Nigg, D., Müller, M., Martinez, E.A., Schindler, P., Hennrich, M., Monz, T., Martin-Delgado, M.A., Blatt, R.: Quantum computations on a topologically encoded qubit. Science **345**(6194), 302–305 (2014)
3. Ofek, N., Petrenko, A., Heeres, R., Reinhold, P., Leghtas, Z., Vlastakis, B., Liu, Y., Frunzio, L., Girvin, S.M., Jiang, L., Mirrahimi, M., Devoret, M., Shoelkopf, R.: Extending the lifetime of a quantum bit with error correction in superconducting qubits. Nature **536**, 441–445 (2016)
4. Sarovar, M., Proctor, T., Rudinger, K., Young, K., Nielsen, E., Blume-Kohout, R.: Detecting crosstalk errors in quantum information processors. Quantum **4**, 321 (2020)
5. Harper, R., Flammia, S.T., Wallman, J.J.: Efficient learning of quantum noise. Nat. Phys. **16**, 1184–1188 (2020)
6. Rivas, A., Huelga, S.F., Plenio, M.B.: Quantum non-Markovianity: characterization, quantification and detection. Rep. Prog. Phys. **77**, 094001 (2014)
7. de Vega, I., Alonso, D.: Dynamics of non-Markovian open quantum systems. Rev. Mod. Phys. **89**, 015001 (2017)
8. White, G.A.L., Hill, C.D., Pollock, F.A., Hollenberg, L.C.L., Modi, K.: Demonstration of non-Markovian process characterization and control on a quantum processor. Nat. Commun. **11**, 6301 (2020)
9. Venegas-Li, A.E., Jurgens, A.M., Crutchfield, J.P.: Measurement-induced randomness and structure in controlled qubit processes. Phys. Rev. E **102**, 040102 (2020)
10. Jurgens, A., Crutchfield, J.P.: Shannon entropy rate of hidden Markov processes. J. Stat. Phys. **183**(32), 1–18 (2020)
11. Jurgens, A., Crutchfield, J.P.: Divergent predictive states: the statistical complexity dimension of stationary, ergodic hidden Markov processes. Chaos **31**(8), 0050460 (2021)
12. Jurgens, A., Crutchfield, J.P.: Ambiguity rate of hidden Markov processes. Phys. Rev. E **104**, 064107 (2021)
13. Crutchfield, J.P., Young, K.: Inferring statistical complexity. Phys. Rev. Lett. **63**, 105–108 (1989)
14. Shalizi, C.R., Crutchfield, J.P.: Computational mechanics: pattern and prediction, structure and simplicity. J. Stat. Phys. **104**, 817–879 (2001)
15. Crutchfield, J.P.: Between order and chaos. Nat. Phys. **8**(January), 17–24 (2012)
16. Parrondo, J., Horowitz, J., Sagawa, T.: Thermodynamics of information. Nat. Phys. **11**, 131–139 (2015)
17. Conte, T., DeBenedictis, E., Ganesh, N., Hylton, T., Strachan, J. Paul., Williams, R.S., Alemi, A., Altenberg, L., Crooks, G.E., Crutchfield, J.P., del Rio, L., Deutsch, J., DeWeese, M.R., Douglas, K., Esposito, M., Frank, M.P., Fry, R., Harsha, P., Hill, M.D., Kello, C., Krichmar, J., Kumar, S., Liu, S.-C., Lloyd, S., Marsili, M., Nemenman, I., Nugent, A., Packard, N., Randall, P., Sadowski, Santhanam, N., Shaw, R., Stieg, A.Z., Stopnitzky, E., Teuscher, C., Watkins, C., Wolpert, D., J. Yang, J., Yufik, Y.: Thermodynamic computing. CoRR, abs/1911.01968 (2019)
18. Gardiner, C., Zoller, P.: Quantum Noise: A Handbook of Markovian and Non-Markovian Quantum Stochastic Methods with Applications to Quantum Optics. Springer, New York (2004)
19. Clerk, A.A., Devoret, M.H., Girvin, S.M., Marquardt, F., Schoelkopf, R.J.: Introduction to quantum noise, measurement, and amplification. Rev. Mod. Phys. **82**, 1155–1208 (2010)
20. Breuer, H.-P., Petruccione, F.: The Theory of Open Quantum Systems. Oxford University Press, Oxford (2007)
21. Rivas, A., Huelga, S.F.: Open Quantum Systems: An Introduction. Springer, Heidelberg (2012)
22. Breuer, H.-P., Laine, E.-M., Piilo, J., Vacchini, B.: Non-Markovian dynamics in open quantum systems. Rev. Mod. Phys. **88**, 021002 (2016)
23. Li, L., Hall, M.J.W., Wiseman, H.: Concepts of quantum non-Markovianity: a hierarchy. Phys. Rep. **759**, 1–51 (2018)

24. Markov, A.A.: Primer statisticheskogo issledovaniya nad tekstom "Evgeniya Onegina", illyustriruyuschij svyaz' ispytanij v cep'. Izv. Akad. Nauk, SPb **93**, 153–162 (1913)
25. Markov, A.A.: Ischislenie veroyatnostej. Spb, 1900; 2-e izd., spb, 1908 edition, 1913. Translated into German, Wahrscheinlichkeits-Rechnung, Teubner, Leipzig-Berlin, 1912; 3-e izd., SPb, 1913; 4-e izd., Moskva, (1924)
26. Milz, S., Modi, K.: Quantum stochastic processes and quantum non-Markovian phenomena. PRX Quantum **2**(3), 030201 (2020)
27. Pollock, F.A., Rodríguez-Rosario, C., Frauenheim, T., Paternostro, M., Modi, K.: Non-Markovian quantum processes: complete framework and efficient characterization. Phys. Rev. A **97**, 012127 (2018)
28. Pollock, F.A., Rodríguez-Rosario, C., Frauenheim, T., Paternostro, M., Modi, K.: Operational Markov condition for quantum processes. Phys. Rev. Lett. **120**, 040405 (2018)
29. Taranto, P., Milz, S., Pollock, F.A., Modi, K.: Structure of quantum stochastic processes with finite Markov order. Phys. Rev. A **99**, 042108 (2019)
30. Efros, A., Nesbitt, D.: Origin and control of blinking in quantum dots. Nat. Nanotechnol. **11**, 661–671 (2016)
31. Crutchfield, J.P., Feldman, D.P.: Regularities unseen, randomness observed: levels of entropy convergence. CHAOS **13**(1), 25–54 (2003)
32. Rabiner, L.R., Juang, B.H.: An introduction to hidden Markov models. IEEE ASSP Mag. **3**, 4–16 (1986)
33. Rabiner, L.R.: A tutorial on hidden Markov models and selected applications. IEEE Proc. **77**, 257 (1989)
34. Bechhoefer, J.: Hidden Markov models for stochastic thermodynamics. New. J. Phys. **17**, 075003 (2015)
35. Riechers, P., Crutchfield, J.P.: Spectral simplicity of apparent complexity, Part I: The nondiagonalizable metadynamics of prediction. Chaos **28**, 033115 (2018)
36. Riechers, P., Crutchfield, J.P.: Spectral simplicity of apparent complexity, Part II: Exact complexities and complexity spectra. Chaos **28**, 033116 (2018)
37. Moore, C., Crutchfield, J.P.: Quantum automata and quantum grammars. Theor. Comput. Sci. **237**(1–2), 275–306 (2000)
38. Gier, D.: Stochastic Quantum Information Processing with Separable Qudit Processes. University of California, Ph.D. dissertation (2023)
39. Blackwell, D.: The entropy of functions of finite-state Markov chains. 28, 13–20, Publishing House of the Czechoslovak Academy of Sciences, Prague, 1957. Held at Liblice near Prague from November 28 to 30 (1956)
40. Crutchfield, J.P., Ellison, C.J., Mahoney, J.R.: Time's barbed arrow: irreversibility, crypticity, and stored information. Phys. Rev. Lett. **103**(9), 094101 (2009)
41. Ellison, C.J., Mahoney, J.R., Crutchfield, J.P.: Prediction, retrodiction, and the amount of information stored in the present. J. Stat. Phys. **136**(6), 1005–1034 (2009)
42. Crutchfield, J.P.: The calculi of emergence: computation, dynamics, and induction. Physica D **75**, 11–54 (1994)
43. Marzen, S.E., Crutchfield, J.P.: Nearly maximally predictive features and their dimensions. Phys. Rev. E **95**(5), 051301(R) (2017)
44. Nielsen, M.A., Chuang, I.L.: Quantum Computation and Quantum Information, 10th anniversary Cambridge University Press, Cambridge (2011)
45. Shannon, C.E.: A mathematical theory of communication. Bell Sys. Technol. J. **27**(379–423), 623–656 (1948)
46. Centore, P.M., Vrscay, E.R.: Continuity of attractors and invariant measures for iterated function systems. Can. Math. Bull. **37**(3), 315–329 (1994)
47. Mendivil, F.: A generalization of IFS with probabilities to infinitely many maps. Rocky Mt. J. Math. **28**(3), 1043–1051 (1998)
48. Kloeckner, B.: Optimal transportation and stationary measures for Iterated Function Systems. In: Mathematical Proceedings (2021). https://hal.archives-ouvertes.fr/hal-02276750
49. Ivanovic, I.D.: How to differentiate between non-orthogonal states. Phys. Lett. A **123**(6), 257–259 (1987)
50. Dieks, D.: Overlap and distinguishability of quantum states. Phys. Lett. A **126**(5), 303–306 (1988)
51. Peres, A.: How to differentiate between non-orthogonal states. Phys. Lett. A **128**(1), 19 (1988)
52. Feldman, D.P., McTague, C.S., Crutchfield, J.P.: The organization of intrinsic computation: complexity-entropy diagrams and the diversity of natural information processing. CHAOS **18**(4), 043106 (2008)
53. Sinai, J.G.: On the notion of entropy of a dynamical system. Dokl. Akad. Nauk. SSSR **124**, 768 (1959)
54. Cover, T.M., Thomas, J.A.: Elements of Information Theory. Wiley, New York (1991)
55. Falkhausen, M., Reininger, H., Wolf, D.: Calculation of distance measures between hidden Markov models. In: EUROSPEECH (1995)
56. Sahraeian, S.M.E., Yoon, B.-J.: A novel low-complexity HMM similarity measure. IEEE Signal Proc. Lett. **18**(2), 87–90 (2011)

57. Zeng, J., Duana, J., Wu, C.: A new distance measure for hidden Markov models. Expert Syst. Appl. **37**(2), 1550–1555 (2010)
58. Riechers, P.M., Crutchfield, J.P.: Beyond the spectral theorem: decomposing arbitrary functions of non-diagonalizable operators. AIP Adv. **8**, 065305 (2018)
59. Crosswhite, G.M., Bacon, D.: Finite automata for caching in matrix product algorithms. Phys. Rev. A **78**, 012356 (2008)
60. Schön, C., Solano, E., Verstraete, F., Cirac, J.I., Wolf, M.M.: Sequential generation of entangled multiqubit states. Phys. Rev. Lett. **95**(11), 110503 (2005)
61. Schön, C., Hammerer, K., Wolf, M.M., Cirac, J.I., Solano, E.: Sequential generation of matrix-product states in cavity QED. Phys. Rev. A **75**(3), 032311 (2007)
62. Marzen, S., Crutchfield, J.P.: Structure and randomness of continuous-time discrete-event processes. J. Stat. Phys. **169**(2), 303–315 (2017)
63. Gu, M., Wiesner, K., Rieper, E., Vedral, V.: Quantum mechanics can reduce the complexity of classical models. Nat. Commun. **3**(762), 1–5 (2012)
64. Mahoney, J.R., Aghamohammadi, C., Crutchfield, J.P.: Occam's quantum strop: synchronizing and compressing classical cryptic processes via a quantum channel. Sci. Rep. **6**, 20495 (2016)
65. Riechers, P.M., Mahoney, J.R., Aghamohammadi, C., Crutchfield, J.P.: Minimized state-complexity of quantum-encoded cryptic processes. Phys. Rev. A **93**(5), 052317 (2016)
66. James, R.G., Mahoney, J.R., Ellison, C.J., Crutchfield, J.P.: Many roads to synchrony: natural time scales and their algorithms. Phys. Rev. E **89**, 042135 (2014)
67. Taranto, P., Pollock, F.A., Milz, S., Tomamichel, M., Modi, K.: Quantum Markov order. Phys. Rev. Lett. **122**, 140401 (2019)
68. Milz, S., Egloff, D., Taranto, P., Theurer, T., Plenio, M.B., Smirne, A., Huelga, S.F.: When is a Non-Markovian quantum process classical? Phys. Rev. X **10**, 041049 (2020)
69. Basharin, G.P., Langville, A.N., Naumov, V.A.: The life and work of A. A. Markov. Linear Algebra Appl. **386**, 3–26 (2004)
70. Markov, A.A.: An example of statistical investigation of the text "Eugene Onegin" concerning the connection of samples in chains. Sci. Context **19**, 591–600 (2006)
71. Ara, P.M., James, R.G., Crutchfield, J.P.: The elusive present: hidden past and future dependence and why we build models. Phys. Rev. E **93**(2), 022143 (2016)